Icarus 219 (2012) 534–555

Contents lists available at SciVerse ScienceDirect

Icarus

journal homepage: www.elsevier.com/locate/icarus

Investigating magnetospheric interaction effects on Titan's ionosphere with the Cassini orbiter Ion Neutral Mass Spectrometer, Langmuir Probe and magnetometer observations during targeted flybys

J.G. Luhmann [a,*], D. Ulusen [a], S.A. Ledvina [a], K. Mandt [b], B. Magee [b], J.H. Waite [b], J. Westlake [c], T.E. Cravens [d], I. Robertson [d], N. Edberg [e], K. Agren [e], J.-E. Wahlund [e], Y.-J. Ma [f], H. Wei [f], C.T. Russell [f], M.K. Dougherty [g]

[a] Space Sciences Laboratory, University of California, 7 Gauss Way, Berkeley, CA 94720, USA
[b] Southwest Research Institute, 6220 Culebra Road, San Antonio, TX 78238, USA
[c] Department of Physics and Astronomy, University of Texas at San Antonio, San Antonio, TX 78249, USA
[d] Department of Physics and Astronomy, University of Kansas, Lawrence, KS 66045, USA
[e] Swedish Institute of Space Physics, Box 537, Uppsala, Sweden
[f] IGPP, Slichter Hall, UCLA, Los Angeles, CA 90095, USA
[g] Space and Atmospheric Physics, Imperial College, London SW7 2AZ, United Kingdom

ARTICLE INFO

Article history:
Received 3 March 2011
Revised 25 February 2012
Accepted 13 March 2012
Available online 30 March 2012

Keywords:
Titan
Titan, atmosphere
Saturn, satellites

ABSTRACT

In the ~6 years since the Cassini spacecraft went into orbit around Saturn in 2004, roughly a dozen Titan flybys have occurred for which the Ion Neutral Mass Spectrometer (INMS) measured that moon's ionospheric density and composition. For these, and for the majority of the ~60 close flybys probing to altitudes down to ~950 km, Langmuir Probe electron densities were also obtained. These were all complemented by Cassini magnetometer observations of the magnetic fields affected by the Titan plasma interaction. Titan's ionosphere was expected to differ from those of other unmagnetized planetary bodies because of significant contributions from particle impact due to its magnetospheric environment. However, previous analyses of these data clearly showed the dominance of the solar photon source, with the possible exception of the nightside. This paper describes the collected ionospheric data obtained in the period between Cassini's Saturn Orbit Insertion in 2004 and 2009, and examines some of their basic characteristics with the goal of searching for magnetospheric influences. These influences might include effects on the altitude profiles of impact ionization by magnetospheric particles at the Titan orbit location, or by locally produced pickup ions freshly created in Titan's upper atmosphere. The effects of forces on the ionosphere associated with both the draped and penetrating external magnetic fields might also be discernable. A number of challenges arise in such investigations given both the observed order of magnitude variations in the magnetospheric particle sources and the unsteadiness of the magnetospheric magnetic field and plasma flows at Titan's (~20Rs (Saturn Radius)) orbit. Transterminator flow of ionospheric plasma from the dayside may also supply some of the nightside ionosphere, complicating determination of the magnetospheric contribution. Moreover, we are limited by the sparse sampling of the ionosphere during the mission as the Titan interaction also depends on Saturn Local Time as well as possible intrinsic asymmetries and variations of Titan's neutral atmosphere. We use organizations of the data by key coordinate systems of the plasma interaction with Titan's ionosphere to help interpret the observations. The present analysis does not find clear characteristics of the magnetosphere's role in defining Titan's ionosphere. The observations confirm the presence of an ionosphere produced mainly by sunlight, and an absence of expected ionospheric field signatures in the data. Further investigation of the latter, in particular, may benefit from numerical experiments on the inner boundary conditions of 3D models including the plasma interaction and features such as neutral winds.

Published by Elsevier Inc.

1. Introduction

In the hierarchy of plasma interactions, Saturn's satellite Titan has traditionally been considered a counterpart to Venus and Mars (e.g. Ma et al., 2008 and references therein); however its location

* Corresponding author.
E-mail address: jgluhman@ssl.berkeley.edu (J.G. Luhmann).

0019-1035/$ - see front matter Published by Elsevier Inc.
http://dx.doi.org/10.1016/j.icarus.2012.03.015

distinguishes it from these other examples of unmagnetized planetary bodies. Cassini flybys of Titan present the opportunity to investigate the (ionospheric) consequences of immersion in a magnetospheric environment. The latter defines the external magnetic field conditions unique to this satellite's orbital location at 20Rs (Rs = Saturn radii), as well as the (subsonic) incident corotating plasma and energetic trapped particle populations. These can affect the ionospheric production, dynamics and spatial distribution. Motivations for such studies also include other aspects of comparative planetology, including atmosphere escape and evolution scenarios. In this paper we consider possible evidence of magnetospheric effects on and in Titan's ionosphere, focusing on 12 close flybys for which in situ ion measurements were obtained by the Cassini Ion Neutral Mass Spectrometer, INMS (Waite et al., 2004), but also considering the larger set of complementary Radio and Plasma Wave Spectrometer (RPWS), Langmuir Probe (LP) electron densities (Gurnett et al., 2004; Wahlund et al., 2005) and magnetic field observations from Cassini's magnetometer (Dougherty et al., 2004). The magnetometer data provide contextual information regarding any organization of the ionospheric properties by magnetic fields of either Saturn or Titan origin.

Unlike its unmagnetized planetary counterparts, Titan's upstream face defined by the magnetosphere's roughly corotating plasma flow is not usually coincident with the dayside hemisphere. As Titan orbits Saturn, the oncoming flow may encounter every combination from the full dayside or nightside ionosphere to partially lit plasma ram faces on either the Saturn-facing side of Titan or the anti-Saturn side (e.g. see Fig. 6 of Waite et al., 2004). Plasma interaction consequences of this separation of controlling coordinate systems were expected, but their relative importance was unclear after the single Voyager flyby. Venus-like draped external fields in the flow wake sampled at ~2.5 Titan radii downstream during the Voyager flyby (e.g. Hartle et al., 1982; Kivelson and Russell, 1983), and similar Cassini observations (e.g. Neubauer et al., 2006; Ma et al., 2006) suggested that Titan produces an induced magnetosphere with an effective conducting obstacle to the surrounding plasma and field of roughly the size of the Titan's cross section. However, Titan's close-in interaction found by Cassini, including the ionosphere, has not been as straightforward to understand.

At Venus, where the solar wind plasma ram always coincides with the subsolar point, the ionosphere, at least at solar maximum, has sufficiently high internal pressure to deflect most of the external plasma and its frozen-in interplanetary field around an ionopause – a pressure balance boundary between the ionosphere and solar wind. Under these conditions the plasma interaction can be well-approximated by MHD simulations of supermagnetosonic solar wind flow against a conducting sphere (e.g. Kallio et al., 1998). Transterminator flows driven by day-to-night thermal pressure gradients in the ionosphere supply a significant nightside ionosphere. The small atmospheric scale height at Venus ensures that solar wind mass-loading effects from planetary ion production and pickup are generally confined to the vicinity of the dayside obstacle boundary. But sometimes the Venus interaction takes on a different character, exhibiting ionospheric magnetization by the draped interplanetary field of the magnetosheath and an apparent cutoff of the transterminator flow source (e.g. Luhmann and Cravens, 1991). Prior to Cassini, several ionospheric models based largely on the expected photochemistry existed (Ip, 1990; Keller et al., 1992; Fox and Yelle, 1997; Galand et al., 1999; Cravens et al., 2004). The close-in Titan plasma interaction was expected to be most similar to Venus conditions for high solar wind dynamic pressure relative to the ionospheric pressure, with some absorption of the incident magnetospheric plasma together with ionospheric penetration by the magnetospheric field (e.g. Keller et al., 1994). The consequences of the magnetospheric particle impacts, compared to the distant Sun's effects, were a matter of speculation based on the Voyager observations far from Titan's ionosphere. Other contributing particle sources, including the corotating ions, newly created Titan pickup ions, and the energetic magnetospheric ions (and neutrals) that create the observed storm-like Titan ENA emissions via charge exchange (Mitchell et al., 2005) have been described by various models (e.g. Garnier et al., 2007; Ledvina et al., 2005; De La Haye et al., 2007; Tseng et al., 2008; Sillanpaa et al., 2007; Cravens et al., 2008), but with the exception of ENA production, not generally verified by observations.

Until Cassini obtained the first in situ electron density measurements with the Langmuir Probe on the first close flyby, TA (Wahlund et al., 2005; Cravens et al., 2005), the main evidence for an ionosphere of Titan was from Voyager radio occultation data (Bird et al., 1997). Cravens et al. (2005) further interpreted the TA data in terms of a mainly solar source, but with a magnetospheric electron source for the unilluminated nightside segment of the pass. Agren et al. (2007) also investigated the nightside ionosphere production by the observed local magnetospheric electrons, concluding it was a viable source in agreement with Cravens et al.'s early assessment. Subsequent analysis of a subset of altitude profile by Galand et al. (2010) also suggested a contribution from magnetospheric electrons. Direct INMS ion measurements were finally obtained on the outbound leg of the fifth targeted flyby (T5), confirming the expected hydrocarbon ion composition (Cravens et al., 2006). This first close Titan pass with both INMS-optimized pointing and ion data acquisition was also analyzed in some detail by De La Haye et al. (2008) who, like Cravens et al., modeled the ion composition assuming both solar and inferred magnetospheric electron impact sources.

The continuing series of targeted close flybys allowed Agren et al. (2009) to analyze electron density profiles from the Langmuir Probe for 17 Titan flybys, solidly establishing that solar photons are the primary ionosphere source above the minimum approach distances of ~950 km. They moreover noted the presence of significant variability of the ionosphere above ~1200 km that they attributed to the plasma interaction, but did not attempt to interpret. By the end of 2009, roughly 60 close (<1200 km altitude, to 950 km) Cassini flybys of Titan had occurred. Of those that featured spacecraft pointing for INMS measurements, about a dozen obtained ionospheric data together with the neutral atmosphere data on at least one leg of the pass.

The body of published work addressing various aspects of the ionospheric observations has continued to grow, with a recent broad review provided by Cravens et al. (2009). The INMS total ion density measurements were found to generally agree with the Langmuir Probe electron densities except at the lowest altitudes (<1100 km) where densities of mass >99 amu ions (the mass limit of the INMS) become important, and at the highest altitudes (>1400 km) where ion flows make accurate measurements problematic (Cravens et al., 2006; Wahlund et al., 2009; Mandt et al., 2011). Robertson et al. (2009) examined selected INMS ionospheric profiles for consistency with solar and magnetospheric electron production models, while Cui et al. (2009) interpreted eight INMS passes to suggest that photochemistry-determined lifetimes are the primary reason for the nighttime profiles' appearance rather than a magnetospheric source. The latter viewpoint is based on the idea that heavy ions at the end of the photochemical chain can survive deep in the upper atmosphere well after direct solar exposure has ended. Another study by Cui et al. (2010) uses averaged ionospheric profiles to consider subjects ranging from ionospheric force balance including magnetic field effects, to escape rates estimated from inferred transterminator ion flows. The present complementary data analyses further investigate what controls Titan's ionosphere. In particular, we examine the ionosphere's appearance as seen by INMS during 12 close Titan flybys, together

with related Langmuir Probe and magnetometer data, for evidence of organization by, or features associated with, the Saturn plasma and field interaction.

As previously mentioned, a challenge in obtaining clear indications of specific magnetospheric effects from so few flybys is the changing geometry of the plasma interaction, coupled with the highly variable conditions at 20 Saturn Radii. Only recently have several authors collected the magnetic field and particle observations along Titan's orbit and analyzed them in a way that provides a better picture of the external conditions that Titan has experienced since Cassini's arrival (e.g. Wei et al., 2009; Rymer et al., 2009; Bertucci et al., 2009; Simon et al., 2010; Thomsen et al., 2010; Garnier et al., 2010). It is important to appreciate that the proximity of Titan's orbit to the magnetopause and near-magnetotail, as well as an apparently variable outer magnetospheric magnetic field (e.g. Wei et al., 2009; Simon et al., 2010), conspire to make each flyby somewhat unique. The magnetospheric plasma flows, while roughly in the corotational direction, are sometimes deflected by magnetospheric dynamics and are generally at subcorotation speeds (e.g. Thomsen et al., 2010). In addition, the behavior of the highly variable energetic particle population (e.g. Sergis et al., 2007, 2009), which contributes a significant part of the external pressure and likely energy input to Titan's atmosphere, is still under investigation (Thomsen et al., 2010). Here we take the view that some useful information may be gained by organizing the data using the main coordinate systems expected to be relevant to the Titan interaction, including the Titan–Sun orbital system, the corotating flow or plasma ram system, and the Titan geographic system. We include many figures in order to simultaneously convey the issues of the sampling biases as well as the conclusions regarding the orderings we find (and do not find).

2. The Titan plasma interaction

The basic physics of a plasma interaction with an unmagnetized planetary body has been described in various reviews (e.g. recently by Ma et al., 2008 and Ledvina et al., 2008). Including a recent paper focused on Titan (Sittler et al., 2010). The key concept of stagnation line pressure balance and transformation starting with the external pressure incident on the obstacle and ending in the sum of obstacle internal pressures has been applied numerous times to understand the basic force balance in such interactions. At Venus, the simplest induced magnetosphere, the average interplanetary magnetic field vector is zero. As a consequence, during the solar maximum observations by the Pioneer Venus Orbiter, a relatively simple picture emerged of evolution from incident solar wind dynamic pressure, to flow and thermal pressure in the shocked solar wind of the magnetosheath, to interplanetary field pileup and its magnetic pressure in the magnetic barrier, to ionospheric pressure planetward of the inner boundary of the barrier or ionopause. The ionospheric pressure consists of its thermal plasma pressure sometimes supplemented by ionospheric field pressure when the solar wind pressure forces the ionopause to the exobase where collisional diffusion of the barrier field sets in (e.g. Elphic et al., 1981; Luhmann and Cravens, 1991). Most of the time around solar maximum, the deep atmosphere and interior of Venus are largely shielded from this external field penetration by currents generated in the ionopause layer. At Mars the interaction is complicated by both the presence of crustal remanent magnetic fields and the smaller scales of the global plasma interaction regions relative to the solar wind proton gyroradius (e.g. Brecht et al., 1993). The crustal fields play a role in the pressure balance that depends on their orientation with respect to the incident solar wind flow and field (Ma et al., 2007), while the standard fluid picture of pressure balance is compromised by the magnetosheath scale and the need to include ion kinetic effects (e.g. Brecht et al., 2000; Simon et al., 2006; Sillanpaa et al., 2007). Titan has aspects of both the Venus and Mars plasma interactions, but its magnetospheric location and orbit around Saturn introduce many special aspects as well.

Fig. 1 illustrates Titan's expected magnetospheric plasma interaction as envisioned from results of both observations of unmagnetized planetary plasma interactions and global modeling. Note that although the ambient magnetic field is shown as North–South in this figure, the observed magnetospheric magnetic field at Titan's orbit during the Cassini mission often has a substantial Saturnward component due to the magnetodisk distortions (Arridge et al., 2008; Wei et al., 2009). Some characteristics that distinguish the Titan interaction are its submagnetosonic nature, and thus absence of a bow shock, and the large scale height of Titan's atmosphere relative to the body radius (e.g. Hartle et al., 2006; Ledvina et al., 2008). In addition, because the interaction is mainly magnetospheric, the external magnetic field has a long-term average orientation. This key difference is expected to produce an Alfven wing-like feature from Saturn's fields that have effectively penetrated the obstacle and form a part of it, as at Io (e.g. Linker et al., 1991; Ma et al., 2008). Although statistical observations of the magnetopause position (Arridge et al., 2006) indicate that Titan's orbit should be located outside of Saturn's magnetopause about 40% of the time at local noon, there are only a few clear examples of Cassini flybys occurring in Saturn's magnetosheath rather than in its magnetosphere (Bertucci et al., 2008; Rymer et al., 2009). These special flybys, one of which has been analyzed in detail and modeled by Ma et al. (2009) and Mueller et al. (2010) are not included in the INMS profiles in the present study.

At Titan, the same issue of finite incident ion gyroradii as mentioned above for Mars applies, but the thick, extended atmosphere nearly doubles the effective size of the obstacle to the external flow relative to the solid body. Early MHD simulations of the Titan plasma interaction predicted that the location of a pressure-balance ionopause at Titan, where external and internal pressures balance, should involve ion-neutral friction forces (Keller et al., 1994). Such conclusions follow when the chain of pressure conversions does not divide itself neatly into internal and external sides above the exobase, which at Titan is located at ~1400 km. In addition, the significant contribution to the external pressure by the suprathermal magnetospheric ion population noted in the introduction (Sergis et al., 2007, 2009; Thomsen et al., 2010) may compromise the direct application of the usual plasma interaction concepts. Nevertheless, selected data comparisons with the global models of the Titan interaction developed in both the MHD (Neubauer et al., 2006; Ma et al., 2006, 2008, 2009; Ulusen et al., 2010) and ion hybrid (Brecht et al., 2000; Simon et al., 2006) limits suggest at least some of the assumptions and approximations in these treatments apply to the real system. It is with all these complications in mind (also see Sittler et al., 2010) that we adopt the simple picture in Fig. 1 as a framework for our investigations and discussions of potential plasma interaction effects on the ionosphere.

Fig. 1 includes shaded/colored areas of the obstacle that have been roughly placed where anticipated energy inputs and ionizing agents are expected to pass through Titan's exobase for a particular Saturn Local Time location. In most cases other than the solar photon input (yellow areas), the details of their spatial and altitude distributions have yet to be confirmed with observations. Proposed magnetospheric sources include magnetospheric electrons (green areas) moving along the magnetospheric field lines that thread the upper atmosphere (e.g. Gan and Cravens, 1992; Agren et al., 2007; Galand et al., 2010), a plasma ram face source (red area) due to the impact of corotating heavy magnetospheric ions that are not deflected above the exobase (e.g. Michael and Johnson,

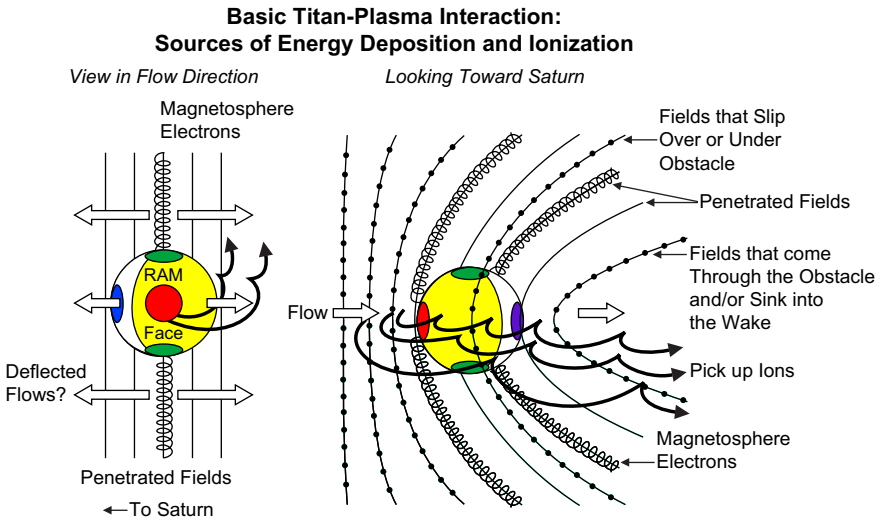

Fig. 1. Schematic of the Titan–magnetosphere interaction indicating possible sources of energy/ionization for the upper atmosphere, as well as the surrounding magnetic field geometry. Titan is expected to have an Io-like Alfven wing as well as draped field lines not connected to the body and a Venus-like induced magnetotail of draped external field. These features, whose details change with the Saturn Local Time location of Titan, are expected to control the access of various surrounding charged particle populations to the atmosphere.

2005; Ledvina et al., 2005; Sillanpaa et al., 2007), a Saturn-face (longitude dependent) incident Titan pickup ion flux (blue area) related to the $E = -V_{plasma} \times B$ electric field from the relative motion of the magnetospheric plasma and field B at V_{plasma} (e.g. Ledvina et al., 2005; Tseng et al., 2008), and corotation wake sources (violet area) from magnetospheric electrons or energetic ions that travel toward Titan along the draped induced magnetotail fields (Keller et al., 1992; Cravens et al., 2008, 2009; Smith et al., 2009) or polar-penetrating Alfven wing fields. The magnetospheric and pickup ion sources should vary with the external conditions including Saturn Local Time and magnetospheric activity levels, but should be relatively fixed in the external flow-oriented coordinate system of Fig. 1.

In addition to the 12 close Titan flybys with INMS ion profiles, parallel analyses of a larger set of ~35 flybys from the Langmuir Probe and magnetometer provide greater context. The three Titan-centered coordinate systems that provide the framework are: Titan Ionospheric Interaction System (TIIS) where the $+x$ axis is defined by the ideal corotation direction; Titan Solar Orbital (TSO) system where the Titan–Sun line is the $+x$ axis; and the Titan geographic system where latitude is measured from Titan's rotation axis and longitude is measured from the Titan meridian facing Saturn. The presence of distinctive features in the collected data for any of these systems, regardless of whether it agrees with our illustration, could be considered a potential detection of a magnetospheric effect.

3. Titan ionosphere in situ observations

Fig. 2 summarizes the flyby geometries for the 12 INMS ion passes analyzed here, which include T5, T17, T18, T26, T36, T39, T40, T48, T50, T51, T57 and T59, where the T# designation identifies the targeted Cassini orbiter Titan flybys. Most of the targeted flybys were either too far from Titan to obtain good ionospheric measurements, or the instruments chosen to control the spacecraft did not include INMS, which must be nearly spacecraft velocity ram-pointed for accurate ion measurements near closest approach, or the ion mode of INMS was not used (see Mandt et al., 2011 for details). In this study we restrict our analysis to INMS measurements below ~1400 km where the pointing and ion sampling conditions are both optimal. Above this altitude, off-pointing and intrinsic ion velocities comparable to the spacecraft velocity compromise the measurements. In addition, the INMS ion densities shown have been multiplied by a factor of three to account for calibration corrections (see Waite et al., 2011 for a detailed discussion).

The flybys in Fig. 2 are plotted in TIIS coordinates which we refer to as the corotation ram system, even though the plasma motion at the orbit of Titan is not strictly along the corotation direction as previously mentioned. The TIIS and Titan geographic systems are best for identifying magnetospheric influences, while the TSO system is best for solar-controlled features. Solar zenith angle ($SZA = a\cos(Xtso/R)$) is typically used for the latter, and an analogous corotation ram zenith angle ($RZA = a\cos(-Xtiis/R)$) for the former. The use of SZA and RZA to organize the observations implies some degree of symmetry around the solar and incident flow axes, respectively. Also implicit in the above discussion is the assumption that the neutral upper atmosphere provides a constant background, which is not strictly the case (e.g. De La Haye et al., 2007; Mueller-Wodarg et al., 2008; Westlake et al., 2011). In addition to potential nonuniform effects of the magnetospheric interaction on the underlying atmosphere e.g. at the Titan poles or where the pickup ions impact (e.g. Sillanpaa et al., 2007), Saturn gravity-produced tides and rotation pole features can introduce geographic dependence. Thus the inclusion of geographic coordinates in the present analysis is warranted as well.

Sparse sampling of the interaction system during the 12 flybys with INMS ion data (Fig. 2a–c), makes the interpretation of the ion measurements in terms of the variable source contributions in Fig. 1 extremely challenging. For altitudes from the closest approaches of ~950–1050 km up to 1400 km, the distribution of sampling in both solar and ram zenith angles is shown in Fig. 3a–c. Most of the ionospheric sampling for these passes is in the flow terminator/flanks around corotation ram zenith angles of 90° (see Fig. 3c). The subsolar, sub-corotation ram ionosphere (small SZA and RZA), and the antisolar, ram wake ionosphere (large SZA and RZA) are poorly sampled by these flybys. Fig. 4a–c shows analogous plots but for Titan geographic coverage. Titan colatitudes are measured from the TIIS $+Z$ axis, and longitude from the TIIS $+Y$ axis (which points toward the center of Saturn). The 12 INMS flybys sample the geographic coordinates in a widely

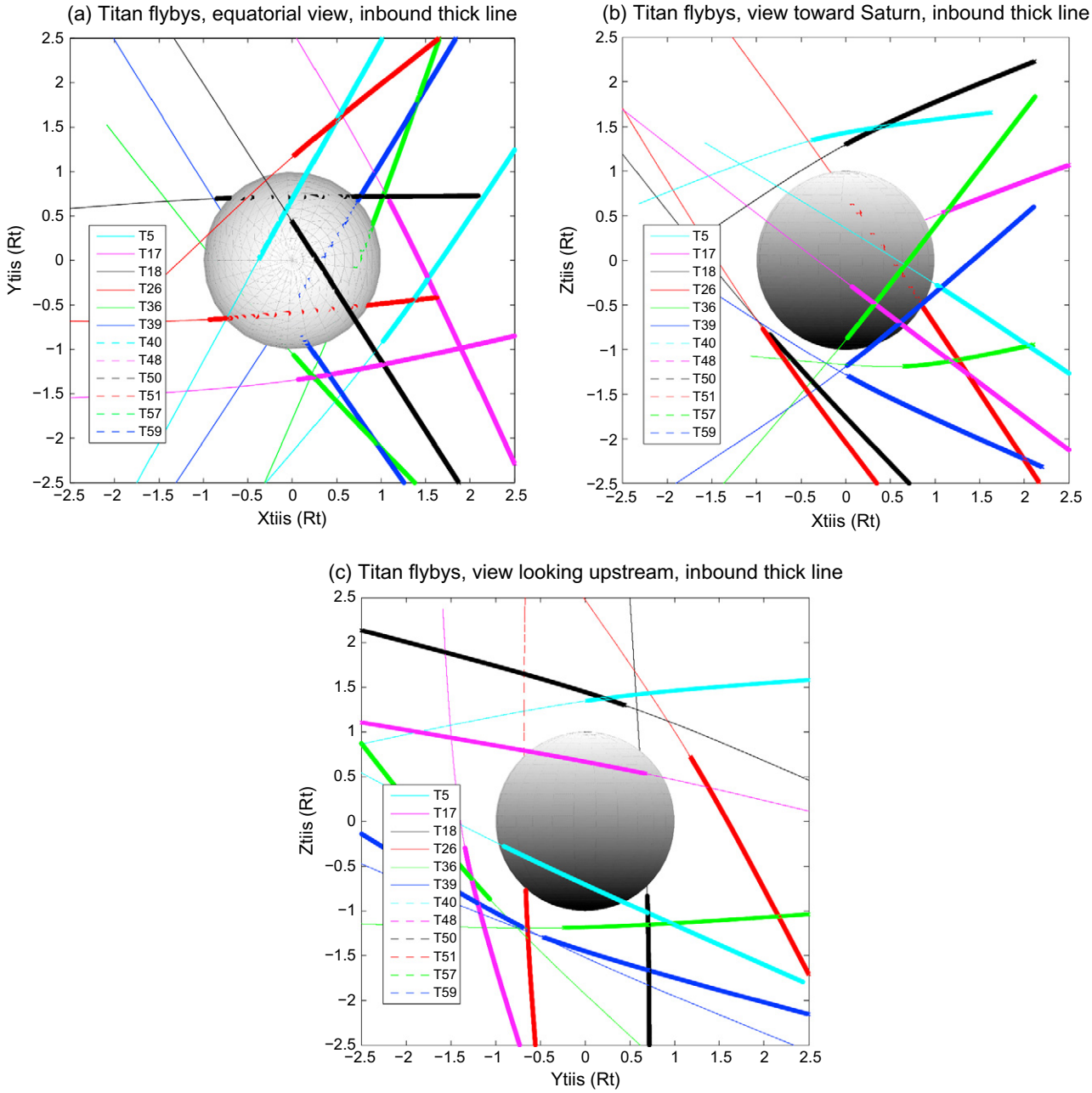

Fig. 2. (a–c) Orthogonal projections, in the TIIS coordinate system of the set of Titan close flybys in 2004–2009 during which Cassini INMS ion data were obtained. In these plots the thick portion of the lines is the inbound leg. (a) Equatorial projection (Xtiis–Ytiis), (b) meridional projection, looking toward Saturn (Xtiis–Ztiis), and (c) view along the corotation flow direction, looking upstream, with Saturn toward the right (Ytiis–Ztiis).

distributed manner. Finally, Fig. 5 shows the Saturn Local Time distribution of these flybys, with four SLT quadrants indicated. While a few INMS ion passes are located near the edges of the sector centered at midnight, most are within the quadrant centered at noon (Group 1). No INMS ion passes were obtained in the dusk quadrant for the period analyzed.

The Cassini Langmuir Probe (Wahlund et al., 2005) does not require specific spacecraft pointing, and therefore obtains a more comprehensive sampling of the Titan ionosphere around most close flybys to higher altitudes than the INMS. As mentioned earlier, a number of detailed studies of the Langmuir Probe (LP) electron densities have already been reported. However these do not provide ion composition information and also do not always include magnetic field analysis. Some features of the ionospheric magnetic field observations are described by Wei et al. (2010b). These include significant variability in field strength and orientation including some structures that resemble large flux ropes. Like the LP data, the magnetometer measurements are generally available throughout the Cassini mission (see Dougherty et al., 2004).

Fig. 6a and b gives an overview of the altitude profiles of the INMS total ion densities from the 12 selected flybys. Colors distinguish inbound (black) from outbound (red) data. For a few of these passes only one leg of data was acquired. In viewing these it is important to remember that the observations are not strictly altitude profiles but represent horizontal traversals of a non-spherically symmetric ionosphere (see Figs. 2–4). As noted earlier, by restricting our study of the INMS data to <1400 km altitudes we avoid measurements that may be compromised by significant ion

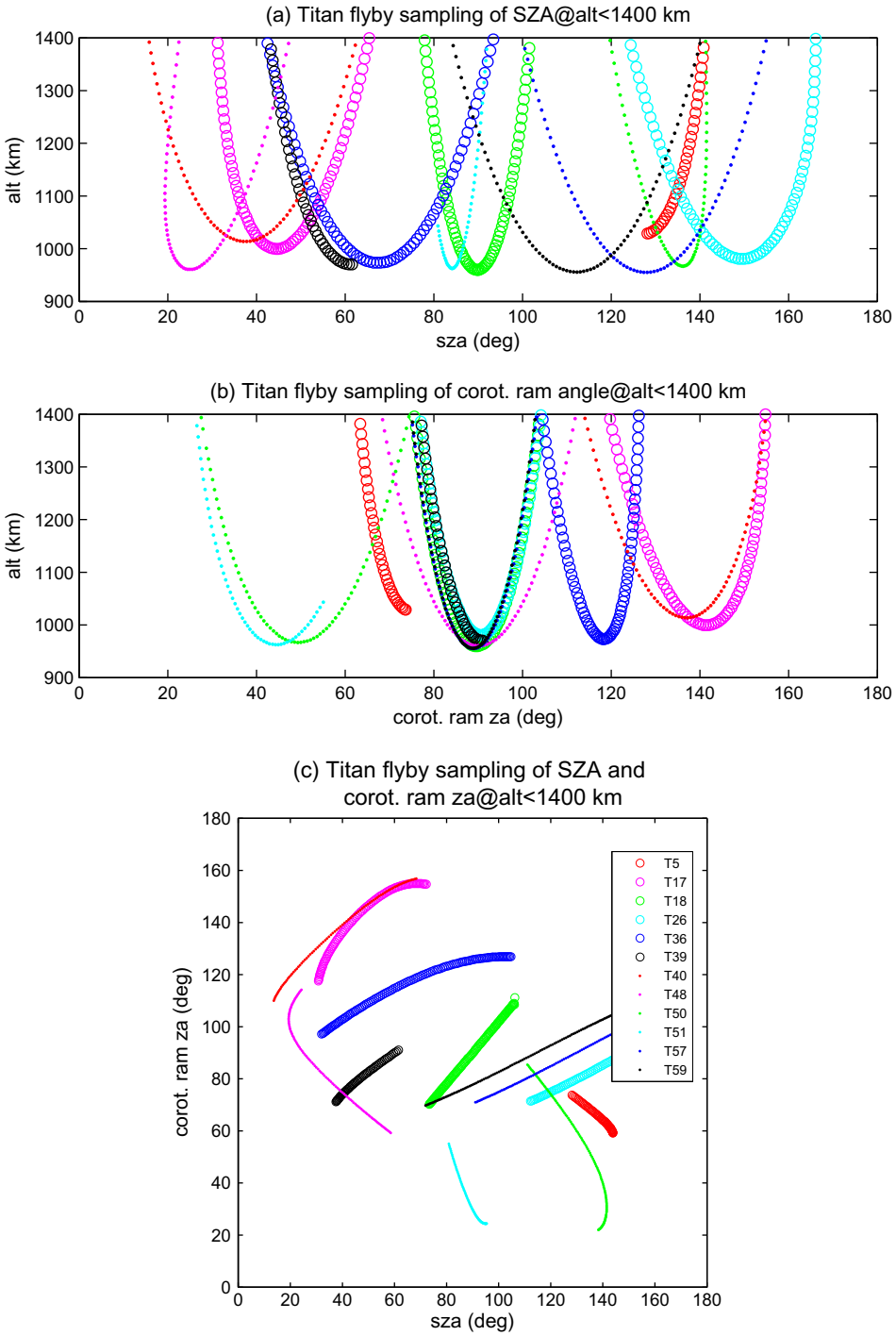

Fig. 3. (a) Solar zenith angle (SZA) and (b) corotation ram zenith angle coverage of the INMS ion flybys vs. altitude. (c) SZA and ram angle coverage. The color key (in (c)) identifies the INMS flybys. (For interpretation of the references to color in this figure legend, the reader is referred to the web version of this article.)

flow velocities relative to the spacecraft, or off-spacecraft ram pointing of the instrument upon entry or egress (see Mandt et al., 2011 for details). The corresponding RPWS Langmuir Probe electron densities (green and cyan points) are shown for comparison. These generally agree with the INMS ion profiles above ~1100 km but then depart from them at lower altitudes where >99 amu ions above the INMS mass range significantly contribute (Wahlund et al., 2009). This agreement adds confidence to both measurements in their middle altitude ranges. A variety of profile appearances is seen, from photochemical or Chapman-layer-like to flattened (e.g. see Cui et al., 2009 for a discussion of the various profile types). Note that the classic Chapman-like profile description does not strictly apply to Titan because its large scale height allows significant solar photoproduction well beyond the terminator (to SZAs ~ 110°). The goal here is to see if these data show organization by considering both the solar and magnetospheric plasma corotation directions, and/or the Titan geographic location.

Another consideration in interpreting the ionospheric profiles is the possible diamagnetic effect of the ionospheric magnetic field. At Venus, the observed ionospheric magnetic and thermal plasma pressures were sometimes comparable, especially under high solar wind pressure conditions. The result is occasional ionospheric

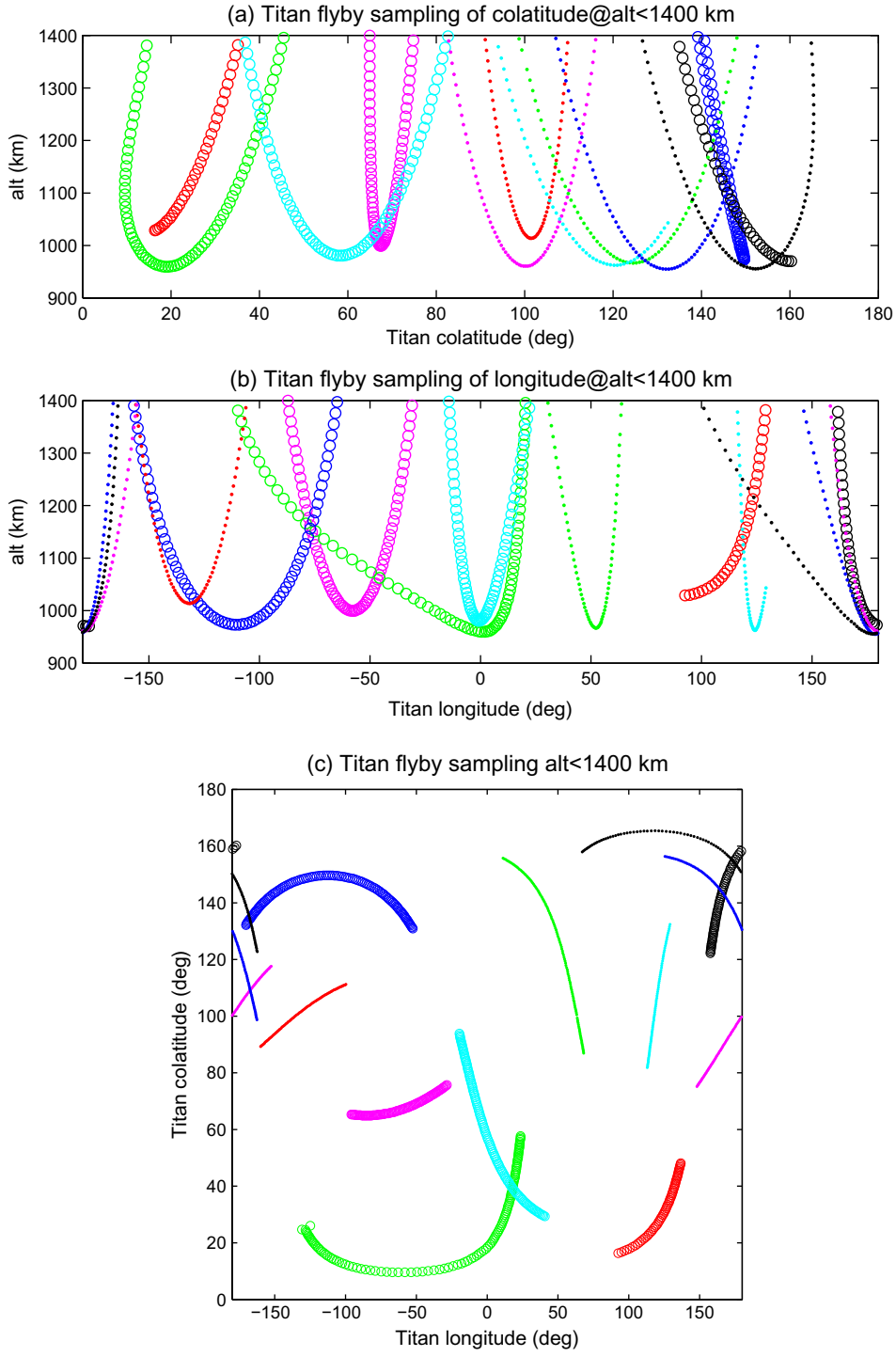

Fig. 4. (a-c) Similar to Fig. 3a–c but for (a) Titan colatitude, (b) Titan longitude, and (c) both geographic angles.

density structure due to pressure balance with the local magnetic field structures, which might be small scale flux ropes or a subsolar belt of penetrated magnetosheath field (e.g. Luhmann and Cravens, 1991). The importance of the ionospheric magnetic pressures in Titan's ionosphere has been estimated by several authors using various assumptions (see Cravens et al., 2010; Cui et al., 2010; Ulusen et al., 2010). However, a visual comparison between the ionospheric density observations in Fig. 6a and b and the corresponding magnetic field magnitude profiles in Fig. 7a and b suggests no obvious relationship between the structure of the measured fields and that in the ionospheric profiles. Here we make no presumptions based on previous analyses of more restricted data sets and simply analyze the magnetic field observations using the same coordinate systems and displays as used for the ionospheric density analyses.

3.1. Large-scale perspective of ionospheric plasma measurements

Fig. 8a and b shows all of the INMS ion measurements from Fig. 6a and b color coded by total density and plotted vs. solar and ram zenith angles in the manner of the trajectory displays in

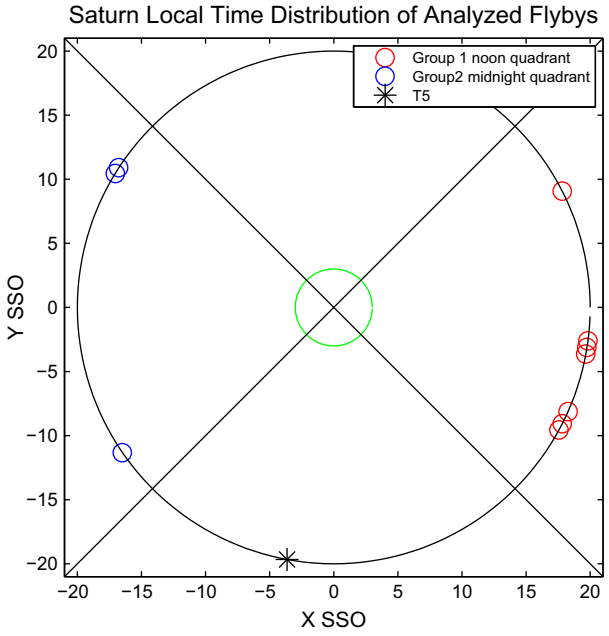

Fig. 5. Saturn Local Time (SLT) locations of the INMS flybys illustrated in Fig. 2a–c. The projection is in the equatorial plane of Saturn in the Saturn Solar Orbital coordinate system (SSO)), where the Sun is along the +Xsso axis toward the right. Four SLT quadrants are identified here. Most of the INMS flybys occurred in the noon SLT quadrant.

Fig. 3a and b. Fig. 8c displays these same data in SZA vs. ram zenith angle only. The solar zenith angle plot in Fig. 8a clearly shows the previously found strong solar control of the total ion density distribution up to 1400 km altitude. Significant ion densities occur beyond the terminator (SZA = 90°) but they are weaker by at least 30%. It is notable that the data with the largest peak densities are also mostly in the corotation wake (e.g. at large ram zenith angles, see Fig. 8b). This raises the possibility that the ionospheric profile may be affected by both direct sunlight and/or by particle precipitation concentrated in the wake at energies such that its ion production peaks at about the same height as the photoionization peak (~1200 km at the solar zenith angles sampled (Fig. 3a)). However, only the presence of the solar source is unambiguous. Plotting the results as a function of both zenith angles (solar and ram) in Fig. 8c reinforces the organizing dominance of SZA. In addition, the ionosphere modeling by Cravens et al. (2005), De La Haye et al. (2008), Robertson et al. (2009) and Cui et al. (2009) using the Titan neutral atmosphere observed by INMS and the solar source assumption confirms that most of the ionization observed on the dayside flybys is produced by solar EUV. From this point on we focus on the seven INMS passes in the noon SLT quadrant (see Fig. 5) in order to eliminate possible ambiguities in interpretation caused by the different (and possibly more variable) external conditions in the midnight sector magnetosphere (e.g. see McAndrews et al., 2009).

Complementary Langmuir Probe data for the noon SLT sector are shown in Fig. 9a–c up to the higher altitudes of 2400 km. As a check, we compared midnight sector Langmuir Probe results to the noon sector results and found only modest differences in general characteristics for most passes. These data include most of the INMS flybys plus an additional ~20 passes. The LP electron densities are color coded using the same scale as the INMS results in Fig. 8a–c. Here the contributions of additional electron density related to heavy ions with mass greater than the INMS limit of 99 amu can be seen at the lowest altitudes. However the general behavior of the densities, including the relatively sharp drop near the terminator, is the same as for the analogous INMS ion data plots in Fig. 8a–c. There are a few passes where the maximum density color (red) appears along a limited part of the trajectory on the nightside, but these are the exception rather than the rule. The complimentary LP sampling in SZA and corotation ram angle, seen by comparing Figs. 8c and 9c, suggests this larger Titan flyby data set is still biased toward the corotation ram system flanks.

The Titan geographic counterparts to Figs. 8 and 9a–c are shown in Figs. 10 and 11a–c. When considered together with the corresponding LP plots in Fig. 11a and b one could argue for a high density bias toward the southern and anti-Saturn hemispheres respectively. It is worth noting that the known departure of the Saturn field from ideally southward at Titan's orbit could move the site of expected energy deposition by the incident ions of either external magnetosphere or atmospheric origin (e.g. Sillanpaa et al., 2007). But there is the caveat that apparent organizations can occur when there are coupled coordinate systems. These biases could be produced simply by the near-coincidence of the dayside and anti-Saturn hemispheres (longitudes <−90° or >90°) in the noon SLT quadrant where the flybys are concentrated. Thus any geographic effect is easily masked by the strong solar control of the ionosphere densities unless it is competitive in a region not dominated by that source. Figs. 10c and 11c suggest that the observed high densities are detected over a broad range of the sampled latitudes and longitudes, but that as usual the sampling is patchy. Nevertheless these results may inspire some revised modeling of ionospheric production and ion energy deposition with more accurate external field orientations.

The issue of the nightside ionosphere character and inferred source(s) is best considered by examining the ion composition measured on INMS (e.g. Cravens et al., 2009a, 2009b; Cui et al., 2009). Figs. 12a–d and 13a–d show four selected ion species (e.g. masses (a) 17, (b) 28, (c) 29, and (d) 79 amu) plotted vs. solar zenith angle and ram zenith angle like the total densities in Fig. 8a and b but again focusing on the noon quadrant flybys. These ions, nominally identified as CH_5^+, $C_2H_5^+$, $HCNH^+$, and $C_6H_7^+$, represent both short and long-lived species, with the heavier ions generally having the longer lifetimes (e.g. Cui et al., 2009). One feature that can be seen in the solar zenith angle sorting (Fig. 12a–d) is that the ion density peak shape and altitude depends on the SZA for the major species, but for the heaviest ions (panel (d)), the lower altitude, lower scale height peak is present across all SZAs consistent with either the long lifetime interpretation or a uniform magnetospheric particle impact source. The same behavior of dayside high density bias for most species is evident in the ram zenith angle-sorted composition data in Fig. 13a–d. The question of whether the more uniformly distributed heavy ion layer is at least partly a result of energetic and fairly isotropic incoming magnetospheric particle sources or purely a consequence of photoion lifetime, or some combination, requires other analyses that include the magnetospheric particle fluxes. Do the corresponding geographic distributions reveal anything about possible latitude dependence or dependence on orientation with respect to Saturn (e.g. longitude)? Figs. 14a–d and 15a–d provide a look, and show that viewed in isolation of other factors, the compositions might suggest hemispheric or longitudinal differences for major ion densities (Figs. 14a–c or 15a–c), but these are subject to the same sampling issues described earlier. Nevertheless they are included to reinforce the different behavior in all respects of the heaviest species shown (Figs. 14d and 15d).

3.2. Large scale perspective of ionospheric magnetic field measurements

Important complementary and contextual information is provided by the ionospheric magnetic field data from the Cassini

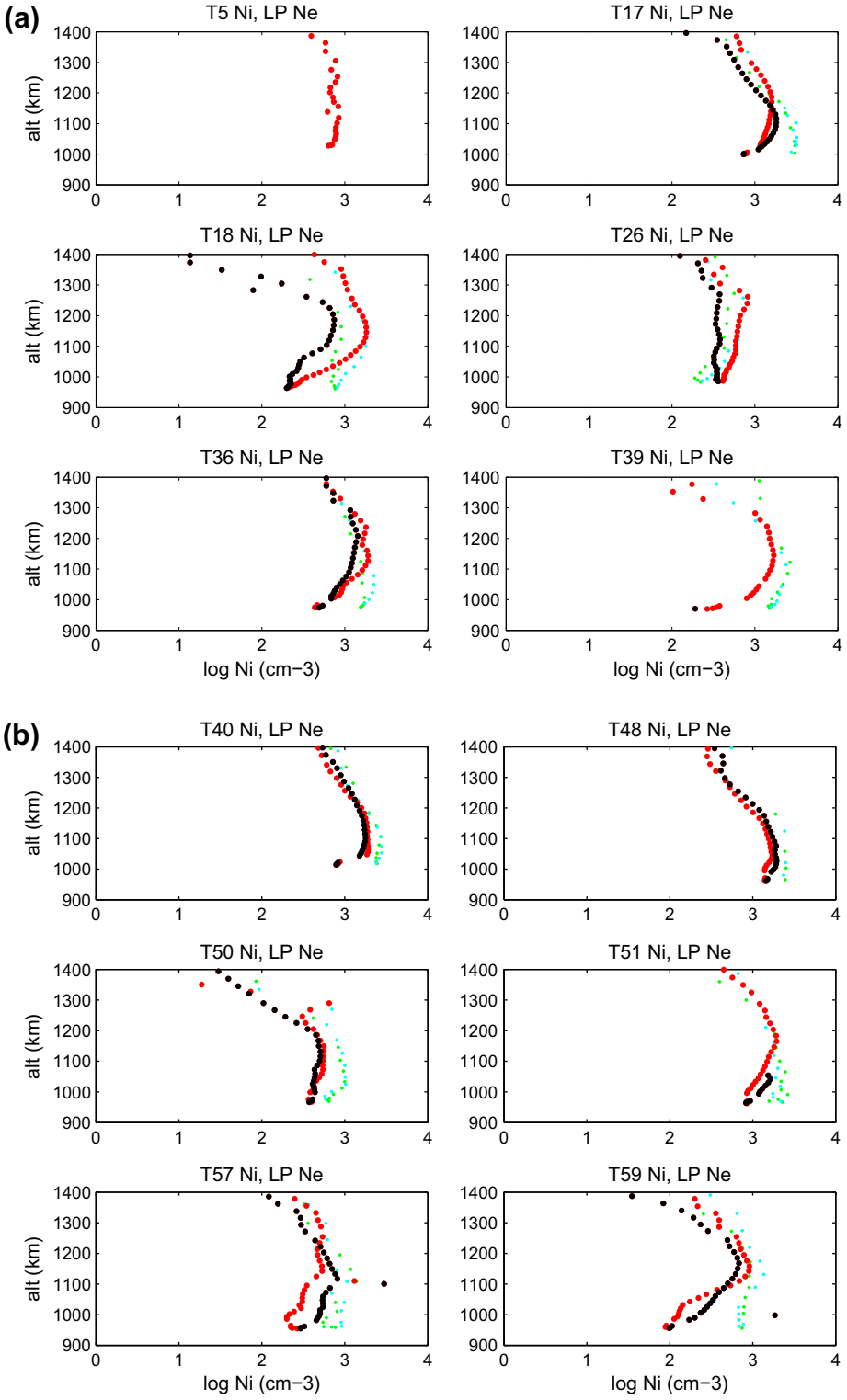

Fig. 6. (a and b) Collected INMS Titan flyby ion density profiles. Black and red points identify the inbound and outbound legs respectively. On several flybys only one leg of ion data was obtained. The green/cyan points show the corresponding Langmuir Probe electron densities measured on the same flybys. (For interpretation of the references to color in this figure legend, the reader is referred to the web version of this article.)

magnetometer (Dougherty et al., 2004) sorted in the same ways as the ions. Here we focus on the total field magnitude and the fractional radial component, as these both have special relevance because of their possible control of diamagnetic effects and ion scale heights, respectively. Fig. 14a–c shows the field magnitude vs. SZA and corotation ram angle, while Fig. 15a–c shows similar displays for the radial component normalized by the field magnitude. The measurements for most of the INMS and LP passes are plotted together for altitudes up to 2400 km. The analogous Titan geographical coordinate plots are shown in Fig. 16a–c for the radial field contributions Br/Btotal. Examples of possible patterns to look for in the magnetic field data, consistent with Fig. 1, include

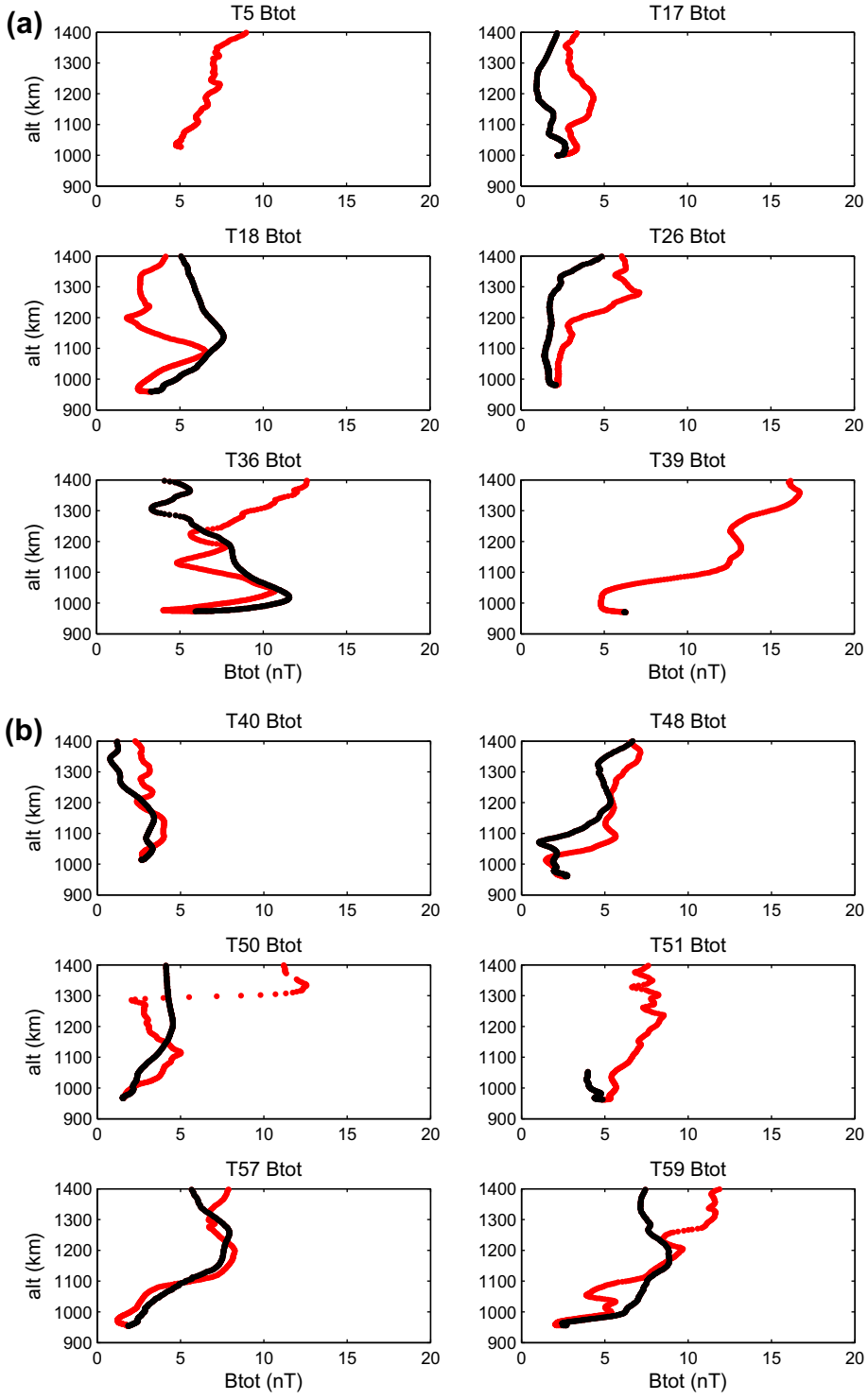

Fig. 7. (a and b) Magnetic field magnitude profiles for the INMS ion flybys in Fig. 6a and b. Black points identify the inbound leg, red points the outbound leg. (For interpretation of the references to color in this figure legend, the reader is referred to the web version of this article.)

corotation ram field pile-up and ordered radial contributions in the geographic polar or corotation wake regions. In particular, if there was a rotation-axis aligned weak dipolar field of Titan that influenced the ionosphere, it could show up as north–south radial field patterns in the geographical system or as consistent tail lobes in the corotation wake.

In striking contrast to the ion and electron density plots from the INMS and LP, the ionospheric magnetic field magnitudes in Fig. 16a–c exhibit relatively weak patterns of behavior, agreeing with what previous authors have found (Wei et al., 2009; Bertucci et al., 2009; Simon et al., 2010). There is a suggestion that the lowest magnetic field magnitudes are generally found at the lowest altitudes sampled, but low fields occasionally occur over the full altitude range. There is also a suggestion of both subsolar and sub-corotation ram (small ram zenith angle) enhancements in the field magnitudes at the higher altitudes, as might be expected

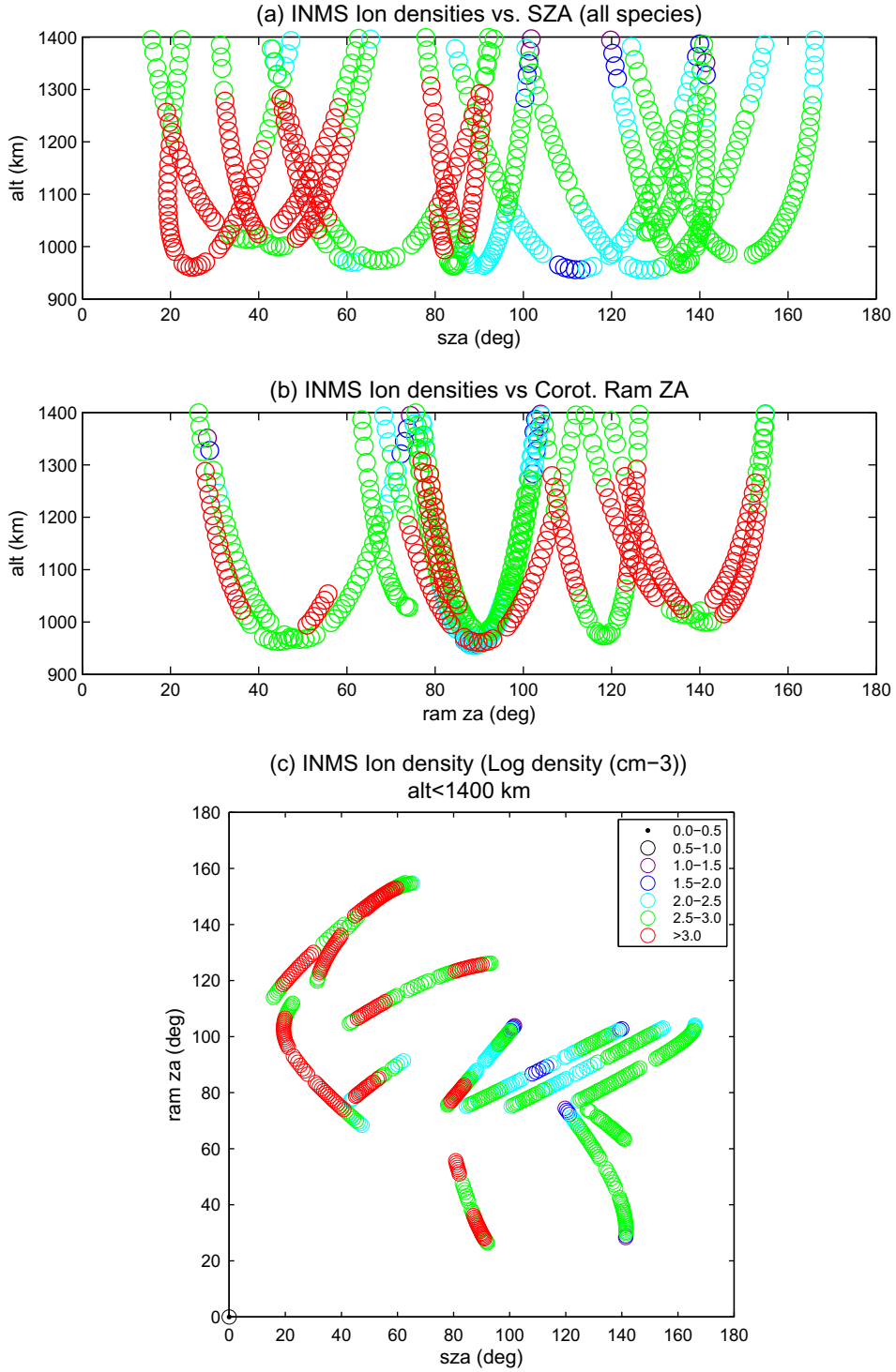

Fig. 8. (a and b) Counterparts to Fig. 5a and b with colors showing log ion (INMS) density in (a) altitude vs. SZA and (b) altitude vs. corotation ram zenith angle displays. The color key is shown in Fig. 8c. (c) INMS ions complement to Fig. 8a and b, highlighting SZA and corotation ram angle dependence together. (For interpretation of the references to color in this figure legend, the reader is referred to the web version of this article.)

from plasma ram compression-related external field pileup and/or field pileup over the dayside ionosphere. This display illustrates that the expected behaviors are only occasionally seen rather than being the norm. The most notable ordering of the ionospheric fields is in the radial component contributions displayed in Fig. 17a–c. In particular Fig. 17c gives the impression of some organization related to solar zenith angle, with positive or outward fields tending to occur on the nightside (large SZAs) and inward radial components near the subsolar region (small SZAs). One might expect a penetrated dipole field of Saturn (see Fig. 1) to reveal itself as latitudinal and hemispheric differences in the radial field strength and sign, with north polar fields inward and south polar fields outward. Yet the geographical coordinate system plots of the radial field fractions in Fig. 18a–c do not show the patterns

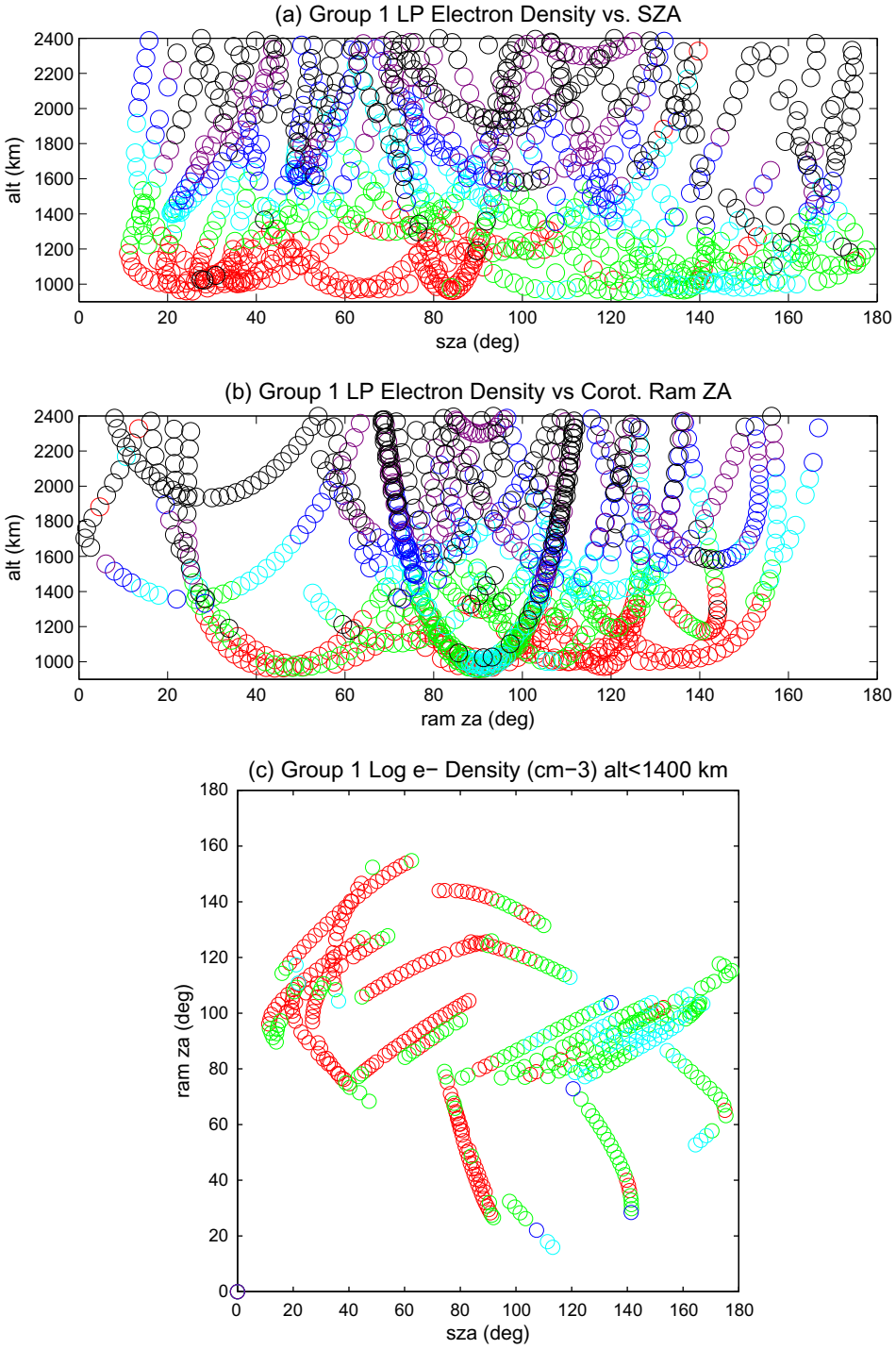

Fig. 9. (a and b) Same as Fig. 8a and b but showing Langmuir Probe (LP) electron density to higher altitudes: (a) altitude vs. SZA and (b) altitude vs. corotation ram zenith angle. Note that the lowest altitude densities here are higher than in Fig. 8a and b because the INMS ion densities do not include mass >99 amu ions which are present in Titan's lower ionosphere. (c) LP densities complement to Fig. 9a and b, highlighting SZA and corotation ram angle dependence together.

consistent with this picture. Instead, the most radial fields at the lowest altitudes are concentrated at midlatitudes. This result presents yet another challenge to models.

4. Discussion

Interpreting the Titan ionospheric observations clearly requires more than a simple cartoon for guidance. However, comparisons to model ionospheres that include the 3D magnetospheric plasma interaction for every flyby with its specific magnetospheric conditions and SLT location is still a major observational and computational challenge. In some cases the incident plasma flow is poorly determined because of spacecraft pointing and instrument field of view limitations. Moreover, it is known to undergo changes in velocity, temperature, direction and composition from flyby to flyby and even during a single flyby (e.g. Thomsen et al., 2010). In addition, there is thought to be an element of time integrated

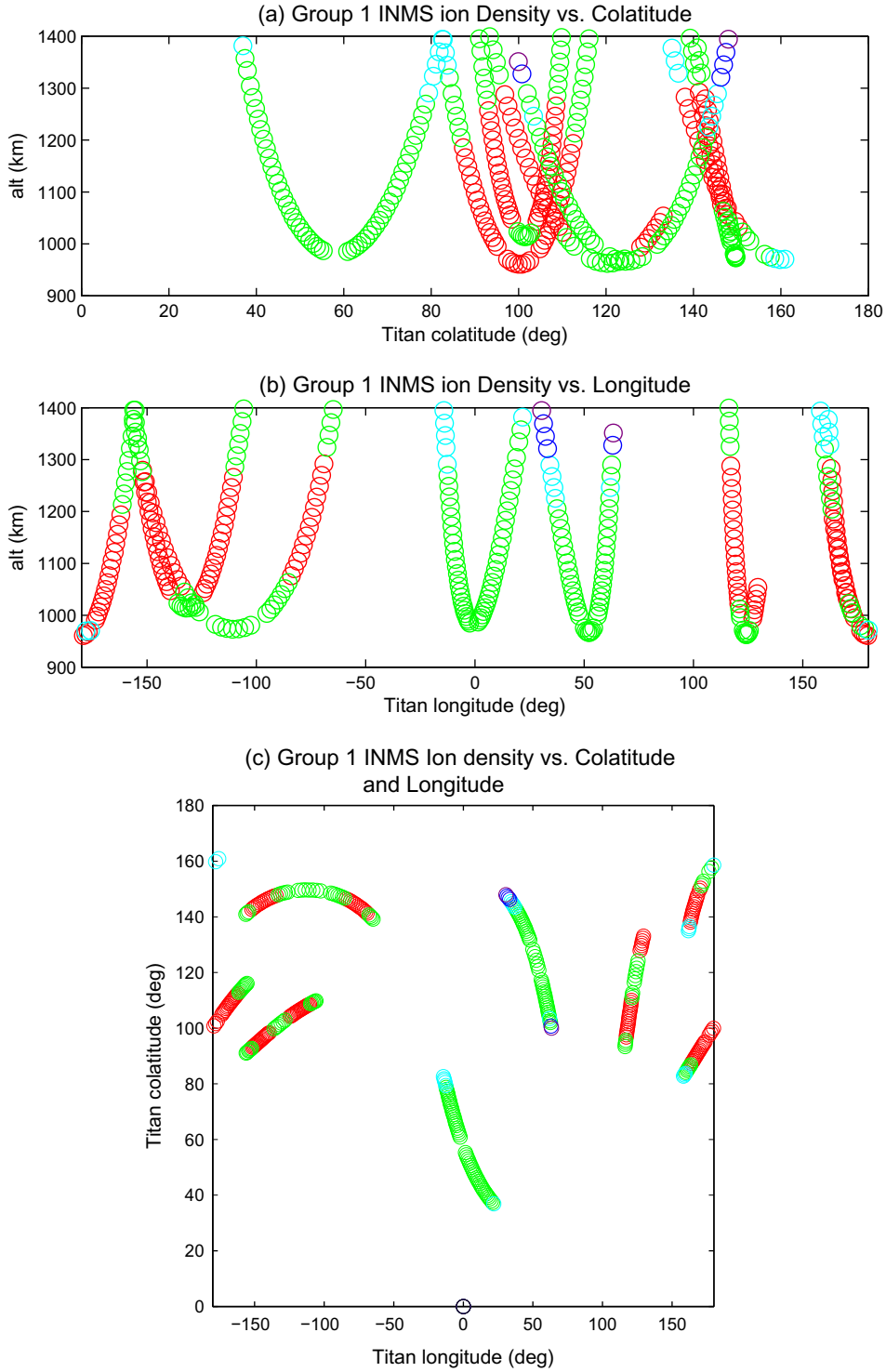

Fig. 10. (a and b) Same as Fig. 8a and b, showing INMS ion densities but for Titan geographic coordinates and eliminating flybys not occurring in the noon SLT quadrant (see Fig. 5). (c) Same as Fig. 8c but for the geographic coordinates, complementing Fig. 10a and b.

behavior involved. Previous explanations for the lack of order in the observed near-Titan magnetic fields include the aforementioned departures of external flow directions from corotation, or 'fossil field' residuals from the occasional passage of Titan into the magnetosheath or times/regions of varying external fields (Bertucci et al., 2008; Simon et al., 2010). For example, Ma et al. (2009) showed that time-dependent external conditions associated with the magnetopause crossing on flyby T32 could have resulted in deeply penetrated remnants of the previously established ionospheric field orientations. These could have persisted for up to hours given the collision rates controlling field dissipation/decay below the exobase (also see Cravens et al., 2010). Titan's ionosphere may constantly be integrating the varying external field, including magnetopause crossings. Alternatively, the neglect of neutral wind effects on the ionosphere dynamics in the may compromise the comparisons with the available models (Cravens

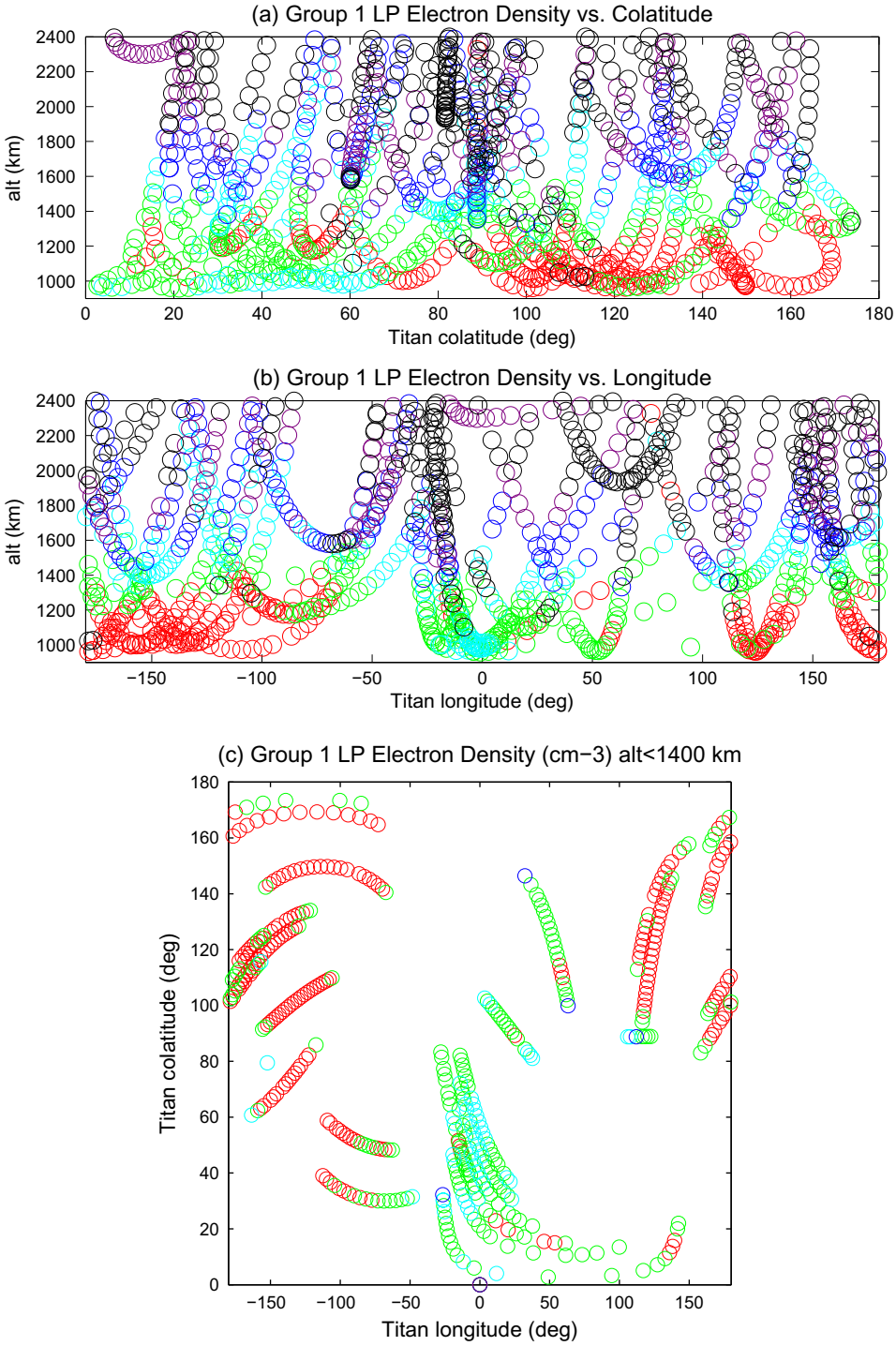

Fig. 11. (a and b) Same as Fig. 9a and b, showing LP electron densities but for Titan geographic coordinates. (c) Same as Fig. 9c, but for the geographic coordinates, complementing Fig. 11a and b.

et al., 2010; Ulusen et al., 2010). Finally, the region between 1400 km and 2400 km is expected to be complicated by a broad boundary layer where much of the main interaction physics takes place (e.g. see Sittler et al., 2010; Ulusen et al., 2012). This is the region where effects of the Titan ion pickup process and instabilities associated with it are expected to be greatest, with uncertain consequences for the magnetic field both locally and below. But this does not explain the apparent ordering in the observed radial components shown in Fig. 17c, or why it disagrees with the general ideas depicted in Fig. 1. As other studies have concluded (e.g. Cravens et al., 2010; Ulusen et al., 2010), some important attributes of the field must be absent in the current model assumptions. Perhaps the key lies in the reason(s) why the persistent dipolar field of Saturn does not reveal itself in at least the latitude distribution of the innermost observed radial field component.

An additional comparison that is useful in this context is between the thermal and magnetic pressures in Titan's ionosphere. Figs. 19a, b, 20a, and b show these comparisons in the solar and

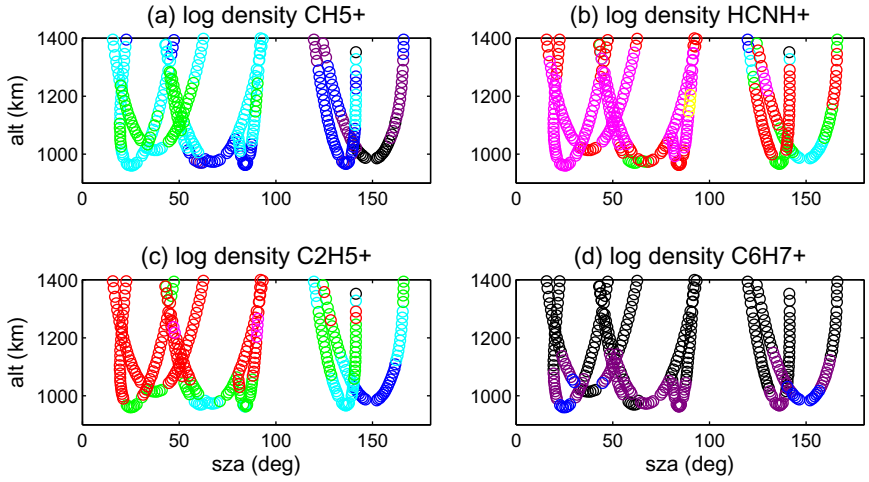

Fig. 12. (a–d) INMS ion density plots showing SZA vs. altitude dependence, but for four INMS ion species (=masses) and using the following log density color code: black = <0.0; blue = 0.0–0.5; cyan = 0.5–1.0; green = 1.0–1.5; red = 1.5–2.0; magenta = 2.0–2.5. (For interpretation of the references to color in this figure legend, the reader is referred to the web version of this article.)

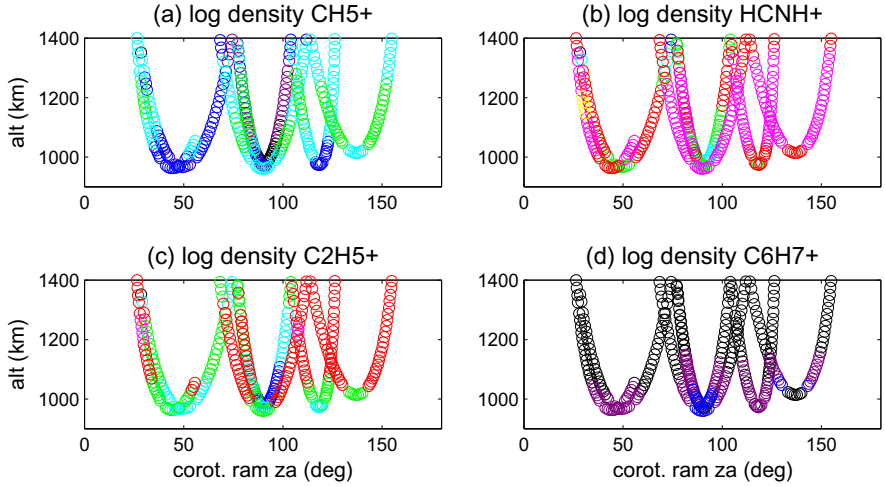

Fig. 13. (a–d) Same as previous plot but showing corotation ram zenith angle vs. altitude dependence for four INMS ion species also using same the color code as in Fig. 12. (For interpretation of the references to color in this figure legend, the reader is referred to the web version of this article.)

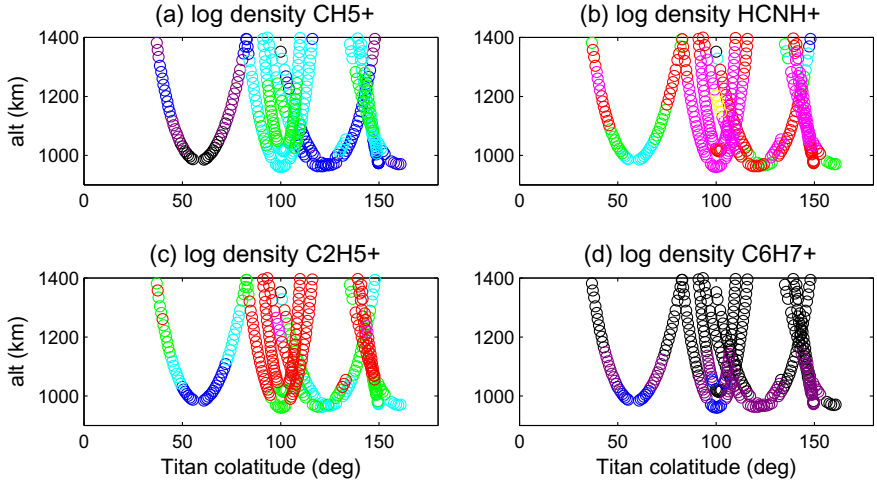

Fig. 14. (a–d) Same as previous plots showing Titan colatitude vs. altitude dependence for four INMS ion species and using the same color code as in Fig. 12. (For interpretation of the references to color in this figure legend, the reader is referred to the web version of this article.)

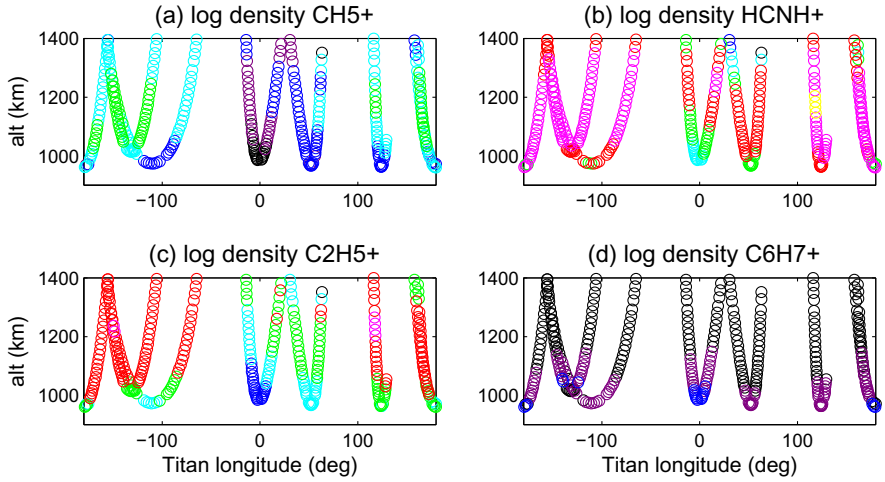

Fig. 15. (a–d) Same as previous plot but showing Titan longitude vs. altitude dependence for four INMS ion species and using the same color code as in Fig. 12. (For interpretation of the references to color in this figure legend, the reader is referred to the web version of this article.)

corotation ram zenith angle display formats used above. For the thermal pressures the LP measurements have been used for the total density and electron temperature, with ion temperatures based on an empirical result from Crary et al. (2009) obtained by combined analysis of INMS and CAPS observations. The thermal pressures in Fig. 19a clearly dominate the dayside ionosphere and are still most significant at night. The corresponding magnetic pressures in Fig. 20a, obtained from the magnetometer measurements of field magnitude, generally become dominant above ~1400 km with the exception of one nearly subsolar pass that detected an exceptionally large magnetic field pressure at 1200–1400 km. This comparison of the thermal and magnetic pressures indicates the plasma thermal pressure holds the greatest influence over the behavior of the dayside ionosphere at <1400 km altitudes. The ionosphere appears to shield out the external field in spite of constant exposure to it. The variability of the external magnetospheric field may be one reason why this shielding effect is maintained. Yet, it is still puzzling why an average field of Saturn at 20Rs does not reveal itself more clearly at least at the lowest altitudes sampled given Titan's long term exposure to it. The ionosphere's ongoing production and convection of the field within it may play some role in this regard. One caveat is that the ion temperature formula used to derive the thermal pressure is based mainly on dayside observations, but was used globally for the purposes of this comparison – thus likely leading to overestimated nightside thermal pressures. In Fig. 20b there is a hint of overall higher field pressures on the sub-corotation ram hemisphere (smaller ram zenith angles) as might be expected for incident flow generated field pileup, while the corresponding thermal pressures in Fig. 19b show a mix of both low and high contributions there. These pressure contrasts, together with the lack of patterns in the radial contributions of the low altitude fields described above, constitute key findings that require further investigation. While the Cassini orbiter will not be able to probe the altitudes below the closest approach distances in the presently available data set, the possibilities for carrying out numerical experiments that connect various inner boundary assumptions with the observed altitude range are steadily improving. These models should at least be able to constrain the possibilities.

5. Concluding remarks

The conclusion of the present study of the collected INMS ion densities from the noon SLT sector of Saturn's magnetosphere, together with complementary Langmuir Probe and magnetometer data, is that the Sun controls Titan's main ionosphere below 1400 km. Any influence of the magnetospheric plasma interaction, with its variable magnetic field and particle populations, is secondary in the dayside observations obtained from Cassini's arrival in 2004 into 2009. The origin(s) of the weaker nightside source(s), e.g. whether transterminator ion transport or magnetospheric particle impact ionization is most important, are not resolvable by the present analysis which only shows a nightside layer consistent with a rather uniform distribution in SZA. The thermal pressure of the ionospheric plasma strongly dominates the dayside, consistent with the idea that the magnetic field is a passive player at these altitudes. To find magnetospheric effects, one has to either study the higher altitudes and/or perform a more detailed analysis of the dependence of the nightside ionosphere on the prevailing local magnetospheric particle fluxes. It is notable that the Cassini mission through 2009 has occurred during one of the deepest solar minima witnessed in modern times, with the lowest average solar EUV fluxes in the space age. Thus one would expect that under more typical solar conditions the solar control of the ionosphere would be even stronger. Of course the magnetosphere, including the magnetopause position, will also change with solar activity. The recent solar minimum was also distinguished by exceptionally low solar wind mass fluxes (McComas et al., 2008) that may have allowed Titan to remain inside Saturn's dayside magnetosphere more of the time than in the previous solar cycles. Such conditions might be expected to have produced a particularly organized plasma interaction picture (e.g. as in Fig. 1) compared to times with stronger solar wind and solar wind disturbances when the subsolar magnetopause crosses 20Rs more often (e.g. Lee et al., 2011).

Titan has been orbiting Saturn since its early stages of formation. Although it has likely been exposed to constantly variable local field conditions, the nearly southward dipolar field of Saturn has probably existed much of that time. If the interior of Titan has some suitably conductive composition, the dipole field at 20Rs should have diffused into it so that it would take hundreds to thousands of years to decay if Titan were removed from the magnetosphere. The field would thus appear as an internal field of Titan with its axis oriented along the Southward direction, imposing that effectively constant inner boundary condition on the Titan plasma interaction. Wei et al. (2009) investigated (their Fig. 2) the statistical behavior of the magnetic field in Saturn's magnetosphere along Titan's orbit as a function of SLT during Cassini's mission. Although there are significant variations about the

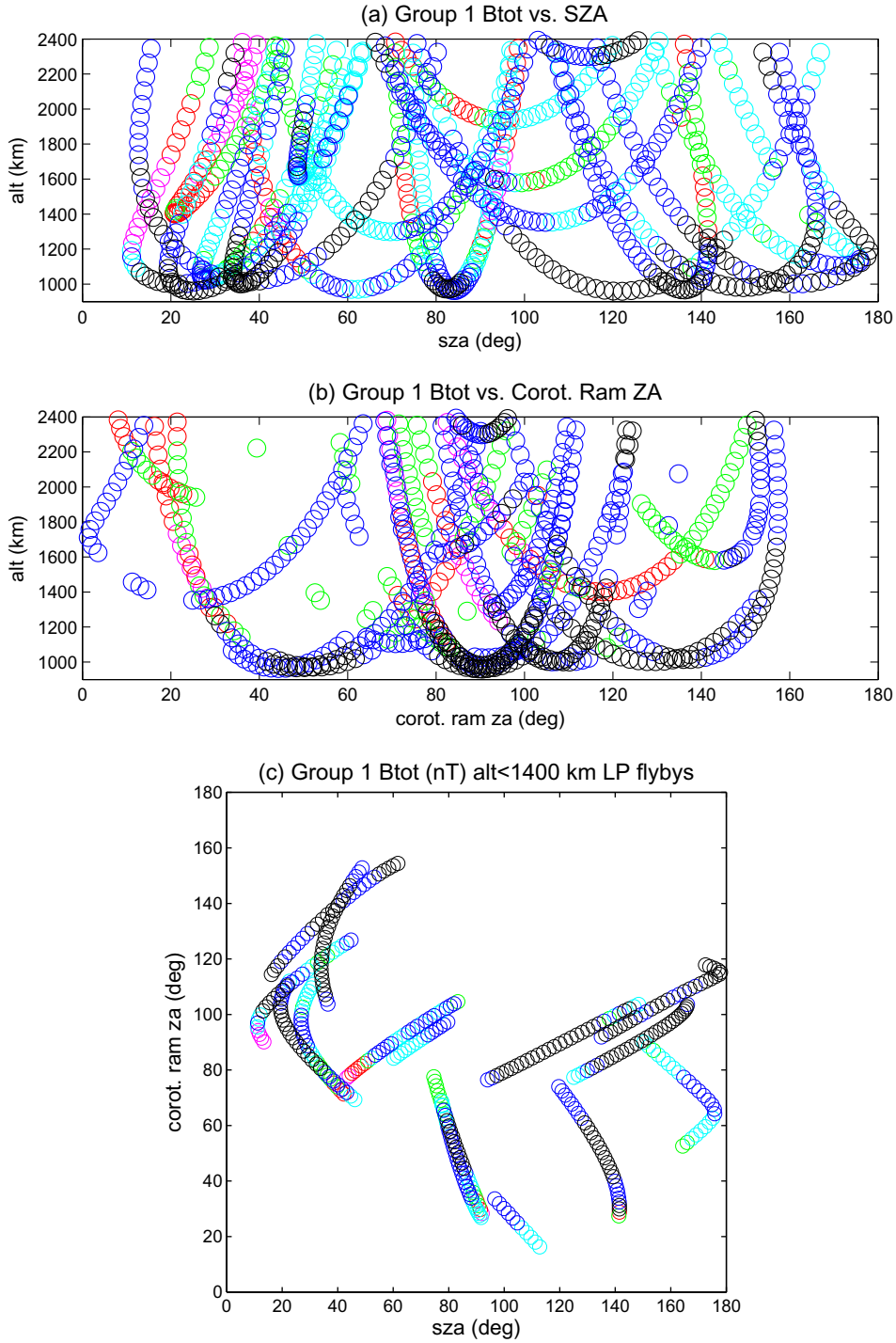

Fig. 16. (a and b) Magnetic field magnitude plots showing the ionospheric field strength dependence on (a) SZA and (b) corotation ram ZA. The color key is shown in (c). Group 1 refers to the Saturn noon quadrant (Fig. 5). This and subsequent field plots include measurements during both INMS and LP passes used in the earlier density plots. (c) Magnetic field magnitudes corresponding to those in (a and b), showing SZA and ram zenith angle dependences. (For interpretation of the references to color in this figure legend, the reader is referred to the web version of this article.)

trends, the near-noon magnetospheric fields are on average nearly Southward, as was observed during Voyager's Titan flyby. The average fields (Brsat, Btsat, Bpsat) in Saturn centered spherical coordinates in the four SLT quadrants of Fig. 5 are 03–09 h (−4.3, 2.3, 2.4); 09–15 h (−1.3, 3.5, 0.3); 15–21 h (−2.1, 2.4, −0.1) (from only three points); 21–03 h (−3.5, 1.7, 1.3). Thus one would expect the noon quadrant (09–15 h) to be compatible with Fig. 1. However, although the majority of INMS ion flybys (see Fig. 5) and all of the LP flybys analyzed here are in the noon quadrant, neither data set has corresponding ionospheric magnetic fields that show the distinctive patterns consistent with Fig. 1. If the southward field geometry in Fig. 1 prevails on the average in this quadrant, one should at least see the radial (with respect to Titan) field components entering Titan's north geographic polar region (small

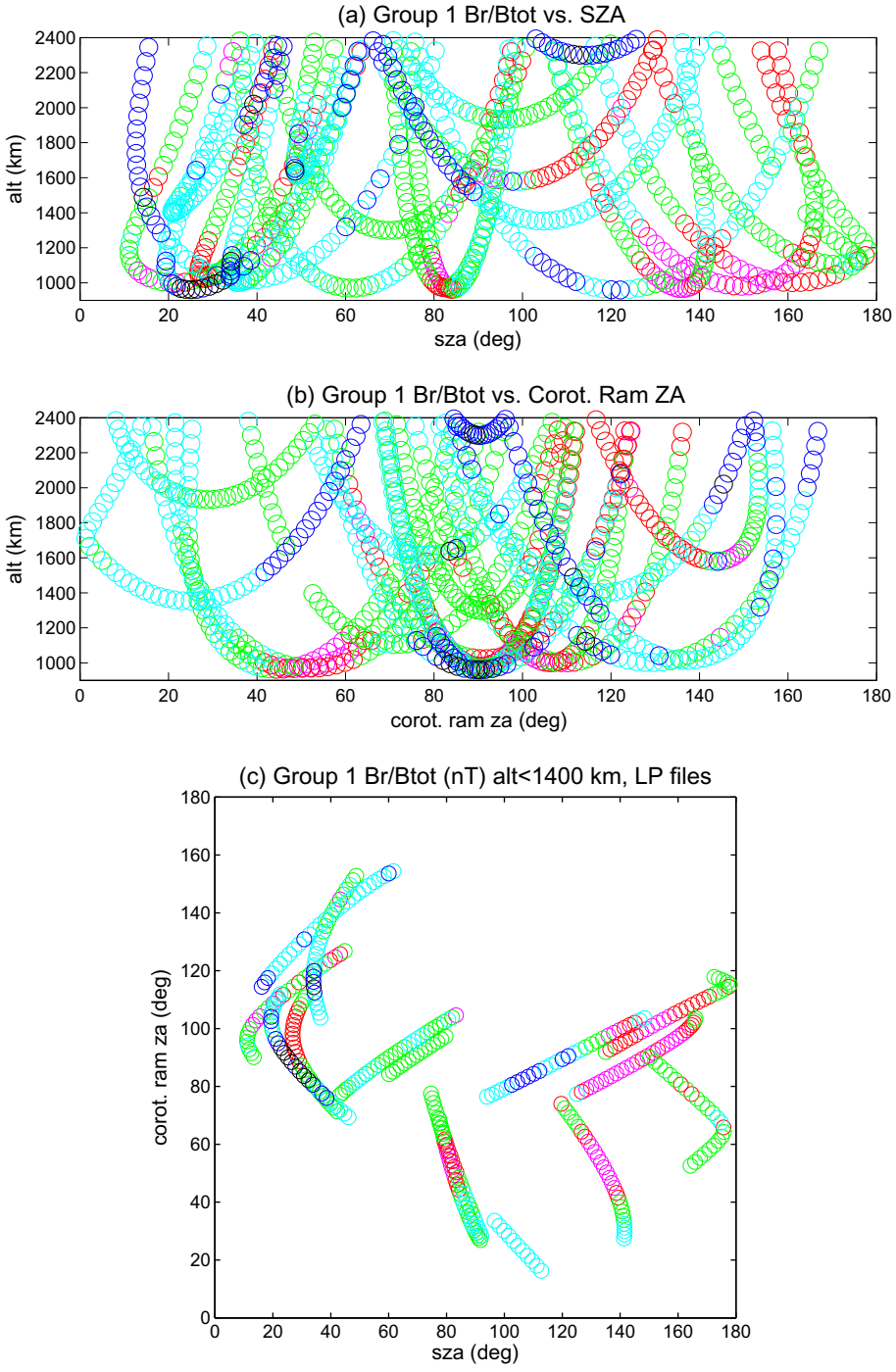

Fig. 17. (a and b) Plots showing the radial field contributions Br/Btot in displays like those in Fig. 16a and b for the field magnitude: (a) altitude vs. SZA and (b) altitude vs. ram ZA. The color key is in (c). (c) Radial field contributions for the flybys in (a and b), showing SZA and ram angle dependences together. (For interpretation of the references to color in this figure legend, the reader is referred to the web version of this article.)

colatitudes) and exiting its south polar region (large colatitudes), with smaller radial fields at mid-low latitudes. But the observations instead show a mixture of radial contributions vs. colatitudes (Fig. 18a and c).

The observed radial fields in the ionosphere of Titan described in this paper are also difficult to reconcile with a simple internal induction picture (e.g. Wei et al., 2010a, 2010b). The relative simplicity of the solar-controlled ionospheric density profiles suggests that the answer lies in the inner boundary conditions on the magnetic field at Titan, or in unmodeled ionospheric currents, rather than the ionospheric properties and sources. Several future numerical experiments would be useful in this regard. The mission-averaged field in Titan's orbit from the analysis of Wei et al. (2009) is (Brsat, Btsat, Bpsat) = (−2.3, 2.9, 0.9). The significant + Ytiis component implied by this average is a result of the bowl-shaped magnetodisk found by the magnetometer (Arridge et al., 2008). If the penetrated field in Fig. 1 has a significant + Ytiis direction, one might try to model the Titan interaction at noon by imposing an external field more nearly in the + Ytiis direction. It may also be informative to try a field that at Titan's surface is the Saturn dipole field, but externally has the magnetospheric large Ytiis component. We note that the bowl shape of the magnetodisk

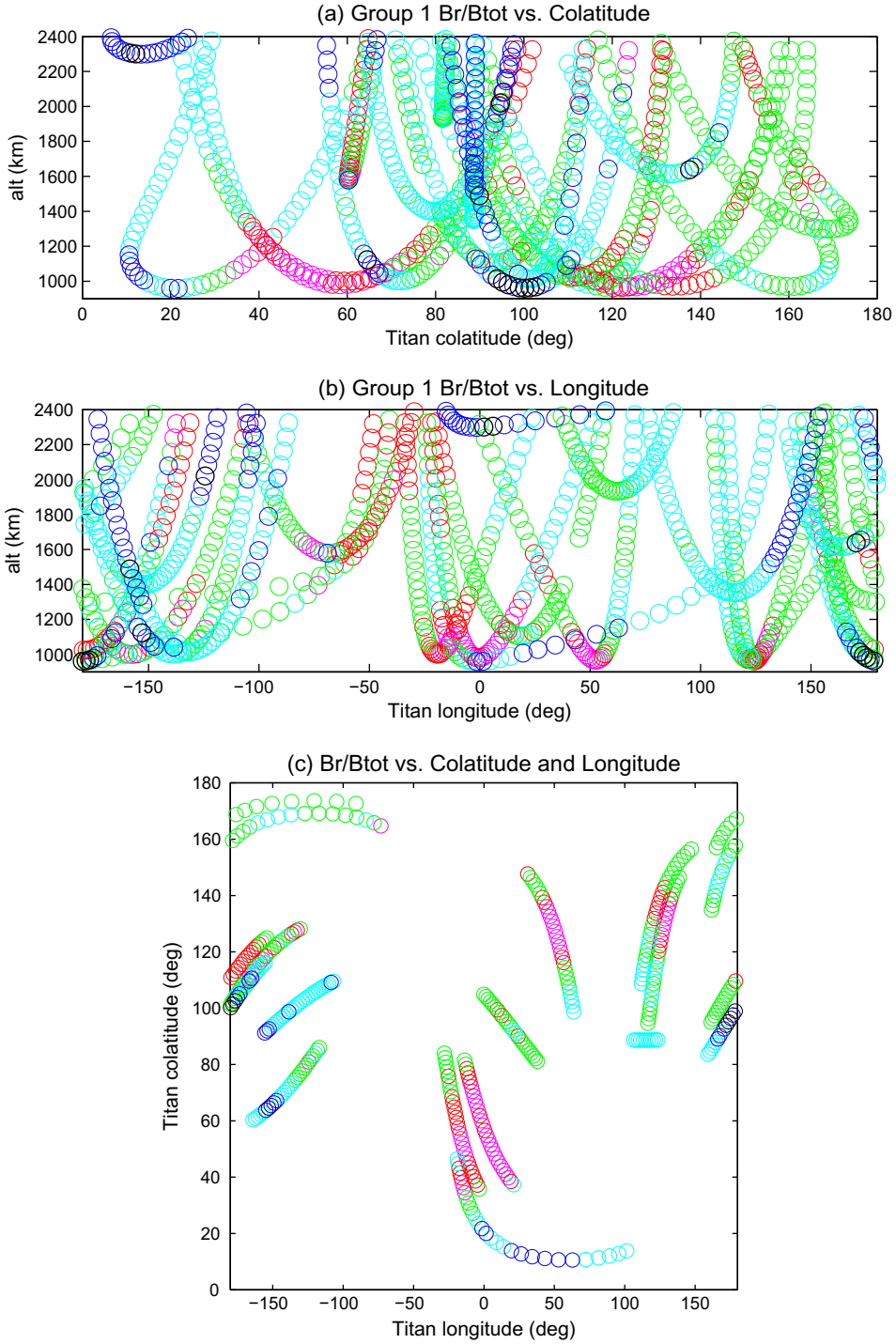

Fig. 18. (a and b) Radial magnetic field contribution plots corresponding to those in Fig. 17a and b, but showing its dependence on Titan colatitude and longitude. The color code is shown in Fig. 17c. (c) Colatitude vs. longitude complement to (a and b). (For interpretation of the references to color in this figure legend, the reader is referred to the web version of this article.)

has flipped over during the recent extended mission, reversing the average + Ytiis component of Titan's external field. Thus the new Titan flyby measurements can be used to see if the radial field in Titan's lower ionosphere has reversed its polarity pattern. Additional numerical experiments could be carried out with the models to investigate the potential effects of significant neutral winds at Titan generating drag forces on the ions and producing associated ionospheric current alterations (e.g. Cravens et al., 2010; Cui et al., 2010; Ulusen et al., 2010). Determining the most correct inner boundary conditions, and their implications, needs to be a key aspect of such efforts given their impacts on model validity and value to data interpretation.

While increasing the statistics of ionospheric sampling during Cassini's extended mission will further constrain the observed patterns of behavior, a Titan orbiter is ultimately necessary to obtain a fuller picture of the energy inputs to the atmosphere and ionosphere and their consequences. In the meantime, other insights can be gained such as the effects of the increasing solar activity and associated EUV fluxes on Titan's environment and ionosphere.

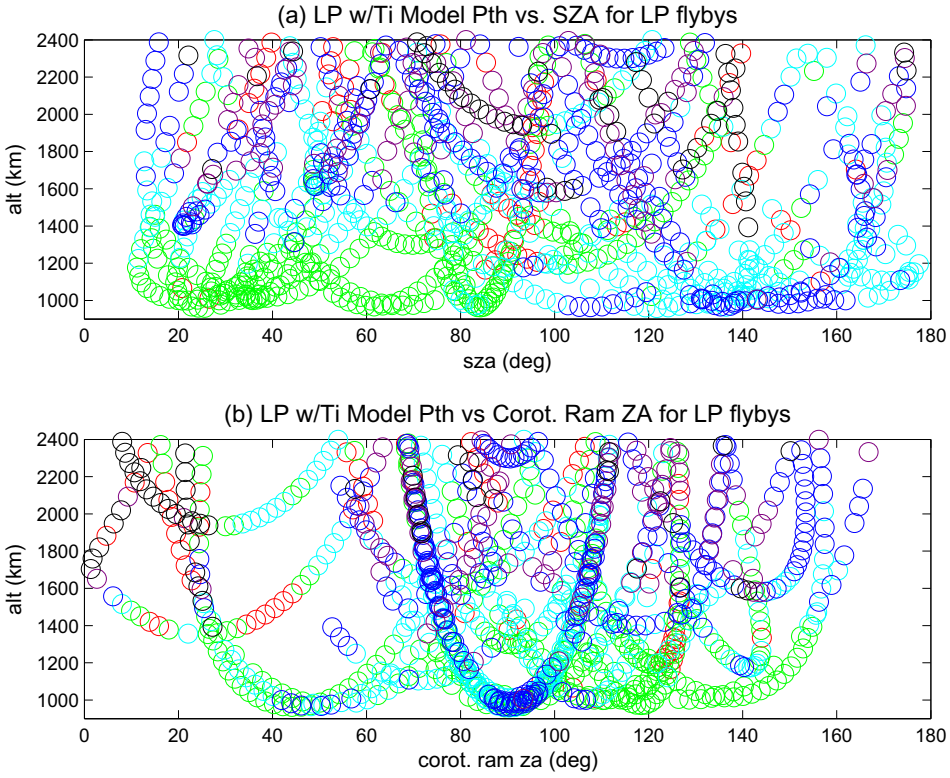

Fig. 19. (a and b) Ionospheric thermal pressure *P*th calculated from the LP measured densities and electron temperatures, together with an ion temperature model derived by Crary et al., 2009 from INMS and CAPS data. The Log pressure (nP) scale is as follows: black: <−2.5, violet: −2.5 to −2.0, blue: −2.0 to −1.5, cyan: −1.5 to −1.0, green: −1.0 to −0.5, red: >−0.5. (For interpretation of the references to color in this figure legend, the reader is referred to the web version of this article.)

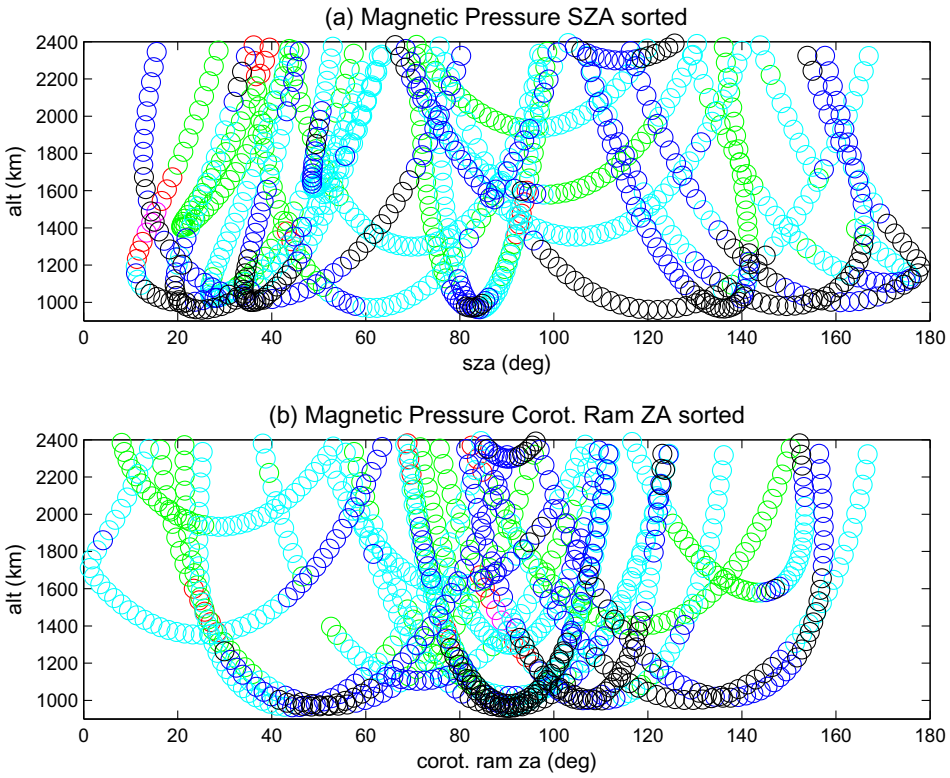

Fig. 20. (a and b) Magnetic field pressure in the ionosphere calculated from the magnetometer measurements of the total field. The pressure scale is the same as in Fig. 19a and b.

Acknowledgments

This work was supported by NASA through the Cassini Project and the INMS investigation team management at SWRI via Subcontract 699080KC. We are grateful to other members of the SWRI data processing team, in particular Dave Gell and Rob Thorpe, as well as Wayne Kasprzak and Hasso Niemann at GSFC for their roles in making the INMS instrument and data available. We are also grateful to the Cassini magnetometer and RPWS LP teams who generously made that data available for this study, and to Roger Yelle, I. Mueller-Wodarg, J. Cui and M. Galand for sharing preprints and helpful discussions.

References

Agren, K. et al., 2007. On magnetospheric electron impact ionization and dynamics in Titan's ramside and polar ionosphere – A Cassini case study. Ann. Geophys. 25, 2359–2369.
Agren, K. et al., 2009. On the ionospheric structure of Titan. Planet. Space Sci. 57, 1821–1827.
Arridge, C.S., Achilleos, N., Dougherty, M.K., Khurana, K.K., Russell, C.T., 2006. Modeling the size and shape of Saturn's magnetopause with variable dynamic pressure. J. Geophys. Res. 111. http://dx.doi.org/10.1029/2005JA011574.
Arridge, C.S. et al., 2008. Saturn's magnetodisc current sheet. J. Geophys. Res. 113. http://dx.doi.org/10.1029/2007JA012540.
Bertucci, C. et al., 2008. The magnetic memory of Titan's ionized ionosphere. Science 321, 1475–1478.
Bertucci, C., Sinclair, B., Achilleos, N., Hunt, P., Dougherty, M.K., Arridge, C.S., 2009. The variability of Titan's magnetic environment. Planet. Space Sci. 57, 1813–1820.
Bird, M.K., Dutta-Roy, R., Asmar, S.W., Rebold, T.A., 1997. Detection of Titan's ionosphere from Voyager 1 radio occultation observations. Icarus 130, 426–436.
Brecht, S.H., Ferrante, J.R., Luhmann, J.G., 1993. Three dimensional simulations of the solar wind interaction with Mars. J. Geophys. Res. 98, 1345–1357.
Brecht, S.H., Luhmann, J.G., Larson, D.J., 2000. Simulation of the Saturnian magnetospheric interaction with Titan. J. Geophys. Res. 105 (13), 119.
Crary, F.J., Magee, B.A., Mandt, K., Waite Jr., J.H., Westlake, J., Young, D.T., 2009. Heavy ions, temperatures and winds in Titan's ionosphere: Combined Cassini CAPS and INMS observations. Planet. Space Sci. 57, 1847–1856.
Cravens, T.E., Vann, J., Clark, J., Yu, J., Keller, C.N., Brull, C., 2004. The ionosphere of Titan: An updated theoretical model. Adv. Space Res. 33, 212–215.
Cravens, T.E. et al., 2005. Titan's ionosphere: Model comparisons with Cassini Ta data. Geophys. Res. Lett. 21. http://dx.doi.org/10.1029/2005GL023249.
Cravens, T.E. et al., 2006. Composition of Titan's ionosphere. Geophys. Res. Lett. 33. http://dx.doi.org/10.1029/2005GL025575.
Cravens, T.E., Robertson, I.P., Ledvina, S., Mitchell, D., Krimigis, S.M., Waite Jr., J.H., 2008. Energetic ion precipitation at Titan. Geophys. Res. Lett. 35. http://dx.doi.org/10.1029/2007GL032451.
Cravens, T.E. et al., 2009a. Model-data comparisons for Titan's nightside ionosphere. Icarus 199, 174–188.
Cravens, T.E., Yelle, R.V., Wahlund, J-E., Shemansky, D.E., Nagy, A.F., 2009b. In: Brown, R., Lebreton, J-P., Waite, J.H. (Eds.), Titan from Cassini–Huygens. Springer, Netherlands, p. 259.
Cravens, T.E. et al., 2010. Dynamical and magnetic field time constants for Titan's ionosphere – Empirical estimates and comparisons with Venus. J. Geophys. Res. 115. http://dx.doi.org/10.1029/2009JA015050.
Cui, J. et al., 2009. Diurnal variations of Titan's ionosphere. J. Geophys. Res. 114. http://dx.doi.org/10.1029/2009JA014228.
Cui, J. et al., 2010. Ion transport in Titan's upper atmosphere. J. Geophys. Res. 115. http://dx.doi.org/10.1029/2009JA014563.
De La Haye, V. et al., 2007. Cassini ion and neutral mass spectrometer data in Titan's upper atmosphere and exosphere: Observations of a suprathermal corona. J. Geophys. Res. 112. http://dx.doi.org/10.1029/226JA012222.
De La Haye, V., Waite Jr., J.H., Cravens, T.E., Robertson, I.P., Lebonnois, S., 2008. Coupled ion and neutral rotating model of Titan's upper atmosphere. Icarus 197, 110–136.
Dougherty, M.K. et al., 2004. The Cassini magnetic field investigation. Space Sci. Rev. 114, 331–383.
Elphic, R.C., Russell, C.T., Luhmann, J.G., Scarf, F.L., Brace, L.H., 1981. The Venus ionopause length scale and controlling factors. J. Geophys. Res. 86 (11430), 11438.
Fox, J.L., Yelle, R.V., 1997. Hydrocarbon ions in the ionosphere of Titan. Geophys. Res. Lett. 24, 2179–2182.
Galand, M., Lilenstein, J., Toublanc, D., Maurice, S., 1999. The ionosphere of Titan: Ideal diurnal and nocturnal cases. Icarus 104, 92–105.
Galand, M. et al., 2010. Ionization sources in Titan's deep ionosphere. J. Geophys. Res. 115. http://dx.doi.org/10.1029/2009JA015100.
Gan, L., Cravens, T.E., 1992. Electrons in the ionosphere of Titan. J. Geophys. Res. 97, 12136–12151.
Garnier, P. et al., 2007. The exosphere of Titan and its interaction with the Kronian magnetosphere. Planet. Space Sci. 55, 165–173.
Garnier, P. et al., 2010. Statistical analysis of the energetic ion and ENA data for the Titan environment. Planet. Space Sci. 58, 1811–1822.
Gurnett, D.A. et al., 2004. The Cassini radio and plasma wave investigation. Space Sci. Rev. 114, 395–463.
Hartle, R.E., Sittler Jr., E.C., Ogilvie, K., Scudder, J.D., Lazarus, A.J., Atreya, S.K., 1982. Titan's ion exosphere observed from Voyager 1. J. Geophys. Res. 87, 1383.
Hartle, R.E. et al., 2006. Initial interpretation of Titan plasma interaction as observed by the Cassini plasma spectrometer: Comparisons with Voyager 1. Planet. Space Sci. 54, 1211–1224.
Ip, W.-H., 1990. Titan's upper ionosphere. Astrophys. J. 362, 354–363.
Kallio, E., Luhmann, J.G., Lyon, J.G., 1998. Magnetic fields near Venus – Comparison between Pioneer Venus Orbiter magnetic field observations and an MHD simulation. J. Geophys. Res. 103, 4723–4737.
Keller, C.N., Cravens, T.E., Gan, L., 1992. A model of the ionosphere of Titan. J. Geophys. Res. 97, 12117–12135.
Keller, C.N., Cravens, T.E., Gan, L., 1994. One dimensional multispecies magnetohydrodynamic models of the ramside ionosphere of Titan. J. Geophys. Res. 99, 6511–6525.
Kivelson, M.G., Russell, C.T., 1983. The interactions of flowing plasmas with planetary atmospheres: A Titan–Venus comparison. J. Geophys. Res. 88, 49.
Ledvina, S.A., Cravens, T.E., Kecskemety, K., 2005. Ion distributions in Saturn's magnetosphere near Titan. J. Geophys. Res. http://dx.doi.org/10.1029/2004JA010771.
Ledvina, S.A., Ma, Y.-J., Kallio, E., 2008. Modeling and simulating flowing plasmas and related phenomena. Space Sci. Rev. 139, 143–189.
Lee, C.O. et al., 2011. Effects of the weaker solar wind observed during the cycle 23 minimum period: Implications for the Titan environment observed on Cassini. Geophys. Res. Lett., submitted for publication.
Linker, J.A., Kivelson, M.G., Walker, R.J., 1991. A three-dimensional MHD simulation of plasma flow past Io. J. Geophys. Res. 96, 21037–21053.
Luhmann, J.G., Cravens, T.E., 1991. Magnetic fields in the ionosphere of Venus. Space Sci. Rev. 55, 201–274.
Ma, Y.-J. et al., 2006. Comparisons between MHD model calculations and observations of Cassini flyby of Titan. J. Geophys. Res. http://dx.doi.org/10.1029/2005JA011481.
Ma, Y.-J. et al., 2007. 3D global multispecies hall-MHD simulation of the Cassini T9 flyby. Geophys. Res. Lett., 34. http://dx.doi.org/10.1029/2007GL031627.
Ma, Y.-J. et al., 2008. Plasma flow and related phenomena in planetary aeronomy. Space Sci. Rev. 139, 311–353.
Ma, Y.-J. et al., 2009. Time-dependent global MHD simulations of Cassini T32 flyby: From magnetosheath to magnetosphere. J. Geophys. Res. 114. http://dx.doi.org/10.1029/2008JA013676.
Mandt, K.E. et al., 2011. Ion densities and ion composition of Titan's upper atmosphere derived by the Cassini Ion Neutral Mass Spectrometer: Analysis methods and model comparisons. J. Geophys. Res., submitted for publication.
McAndrews, H.J. et al., 2009. Plasma in Saturn's nightside magnetosphere and implications for global circulation. Planet. Space Sci. 57, 1714–1722.
McComas, D.J. et al., 2008. Weaker solar wind from the polar coronal holes and the whole Sun. Geophys. Res. Lett., 35. http://dx.doi.org/10.1029/2008GL034896.
Michael, M., Johnson, R.E., 2005. Energy deposition of pickup ions and heating of Titan's atmosphere. Planet. Space Sci. 53, 1510–1514.
Mitchell, D.G., Brandt, P.C., Roelof, E.C., Dandouras, J., Krimigis, S.M., Mauk, B.H., 2005. Energetic neutral atom emissions from Titan interaction with Saturn's magnetosphere. Science 308, 989–992.
Mueller, J. et al., 2010. Magnetic field fossilization and tail reconfiguration in Titan's plasma environment during a magnetopause passage: 3D adaptive hybrid code simulations. Planet. Space Sci. 58, 1526–1546.
Mueller-Wodarg, I.C.F., Yelle, R.V., Cui, J., Waite, J.H., 2008. Horizontal structures and dynamics of Titan's thermosphere. J. Geophys. Res. 113. http://dx.doi.org/10.1029/2007JE003033.
Neubauer, F.M. et al., 2006. Titan's near magnetotail from magnetic field and electron plasma observations and modeling: Cassini flybys TA, TB, and T3. J. Geophys. Res. 111. http://dx.doi.org/10.1029/2006JA011676.
Robertson, I.P. et al., 2009. Structure of Titan's ionosphere: Model comparisons with Cassini data. Planet. Space Sci. 57, 1834–1846.
Rymer, A.M., Smith, H.T., Wellbrock, A., Coates, A.J., Young, D.T., 2009. Discrete classification and energy spectra of Titan's varied magnetospheric environment. Geophys. Res. Lett. 36. http://dx.doi.org/10.1029/2009GL039427.
Sergis, N. et al., 2007. Ring current at Saturn: Energetic particle pressure in Saturn's equatorial magnetosphere measured with Cassini/MIMI. Geophys. Res. Lett. 34. http://dx.doi.org/10.1029/2006GL029223.
Sergis, N. et al., 2009. Energetic particle pressure in Saturn's magnetosphere measured with the Magnetospheric Imaging Instrument on Cassini. J. Geophys. Res. 114, A02214. http://dx.doi.org/10.1029/2008JA013774.
Sillanpaa, I., Kallio, E., Jarvinen, R., Janhunen, P., 2007. Oxygen ions at Titan's exobase in a Voyager 1-type interaction from a hybrid simulation. J. Geophys. Res. 112. http://dx.doi.org/10.1029/2007JA012348.
Simon, S., Bosswetter, A., Bagdonat, T., Motschmann, U., Glassmeier, K.-H., 2006. Plasma environment of Titan: A 3D hybrid simulation study. Ann. Geophys. 24, 1113–1135.
Simon, S. et al., 2010. Titan's highly dynamic magnetic environment: A systematic survey of Cassini magnetometer observations from flybys TA-T62. Planet. Space Sci. 58, 1230–1251.

Sittler, E.J. et al., 2010. Energy deposition processes in Titan's upper atmosphere and its induced magnetosphere. In: Brown, R., Lebreton, J-P., Waite, J.H. (Eds.), Titan from Cassini Huygens. Springer, pp. 393–453.
Smith, H.T., Mitchell, D.G., Johnson, R.E., Paranicas, C.P., 2009. Investigation of energetic proton penetration into Titan's atmosphere using the Cassini INCA instrument. Planet. Space Sci. 57, 1538–1546.
Thomsen, M.F. et al., 2010. Survey of ion plasma parameters in Saturn's magnetosphere. J. Geophys. Res. 115, A10220. http://dx.doi.org/10.1029/2010JA015267.
Tseng, W.-L., Ip, W.-H., Kopp, A., 2008. Exosphere heating by pickup ions at Titan. Adv. Space Res. 42, 54–60.
Ulusen, D., Luhmann, J., Ma, Y.J., Ledvina, S., Cravens, T., Mandt, K., Waite, J.-H., Walund, J.-E., 2010. Investigation of the force balance in Titan's ionosphere: Cassini T5 flyby model/data comparisons. Icarus 210, 867–880.
Ulusen, D., Luhmann, J.G., Ma, Y.-J., Mandt, K.E., Waite, J.H., Dougherty, M.K., Wahlund, J.-E., Russell, C.T., Cravens, T.E., Edberg, N.J., Agrin, K., 2012. Comparisons of Cassini flybys of the Titan magnetospheric interaction with an MHD model: Evidence for organized behavior at high altitudes. Icarus 217, 43–54.
Wahlund, J.E. et al., 2005. Cassini measurements of cold plasma in the ionosphere of Titan. Science 308, 986–989.
Wahlund, J.-E. et al., 2009. On the amount of heavy molecular ions in Titan's ionosphere. Planet. Space Sci. 57, 1857–1865.
Waite Jr., J.H. et al., 2004. The Cassini Ion and Neutral Mass Spectrometer (INMS) investigation. Space Sci. Rev. 114, 113.
Waite Jr., J.H. et al., 2011. In-flight and ground calibration of the Cassini Ion Neutral Mass Spectrometer: Determination of the calibration constant required for calculation of ion and ambient neutral densities and related uncertainties. J. Geophys. Res., submitted for publication.
Wei, H.-Y., Russell, C.T., Wellbrock, A., Dougherty, M.K., Coates, A.J., 2009. Plasma environment at Titan's orbit with Titan present and absent. Geophys. Res. Lett. 36. http://dx.doi.org/10.1029/2009GL041048.
Wei, H.-Y., Russell, C.T., Dougherty, M.K., Neubauer, F.M., Ma, Y.-J., 2010a. Upper limits on Titan's magnetic moment and implications for its interior. J. Geophys. Res. 115. http://dx.doi.org/10.1029/2009JE003538.
Wei, H.-Y., Russell, C.T., Zhang, T.L., Dougherty, M.K., 2010b. Comparison study of magnetic flux ropes in the ionospheres of Venus, Mars and Titan. Icarus 206, 174–181.
Westlake, J. et al., 2011. Titan's thermospheric response to various plasma environments. J. Geophys. Res. 116. http://dx.doi.org/10.1029/2010JA016251.